MtvS Interacts With RNA Polymerase to Regulate the *Francisella* Type V-A CRISPR-Cas System

Maj Brodmann[1], Christian F. Baca[1,2], Joshua Chandanani[3,4], Elizabeth A. Campbell[4] and Luciano A. Marraffini[1,5]

[1] Laboratory of Bacteriology, The Rockefeller University, New York, NY 10065, USA

[2] Tri-Institutional PhD Program in Chemical Biology, Weill Cornell Medical College, Rockefeller University and Memorial Sloan Kettering Cancer Center, New York, NY 10065, USA

[3] Laboratory of Molecular Biophysics, The Rockefeller University, New York, NY 10065, USA

[4] Laboratory of Molecular Pathogenesis, The Rockefeller University, New York, NY 10065, USA

[5] Howard Hughes Medical Institute, The Rockefeller University, New York, NY 10065, USA

Correspondence: mbrodmann@rockefeller.edu, marraffini@rockefeller.edu

Abstract

CRISPR-Cas systems endow bacteria and archaea with adaptive immunity against mobile genetic elements, playing a fundamental role in shaping microbial communities. Many organisms harbor more than one CRISPR-Cas system, and little is known about whether and how they are differentially regulated, in many instances due to the impossibility of studying CRISPR immunity in native hosts. Here we studied the regulation of endogenous type II-B and type V-A CRISPR-Cas systems in opportunistic human pathogen *Francisella novicida* U112. Fluorescence microscopy and transcriptomics experiments revealed that while the type II-B system is constitutively expressed, the type V-A CRISPR-Cas system is differentially expressed at stationary phase and high cell density. Using mass spectrometry and genetics we identified MtvS as a factor required for the differential expression of the type V-A CRISPR-Cas locus. Surprisingly, MtvS-dependent expression of the type V-A CRISPR-Cas system at high cell density is linked to a quorum sensing-like behavior. In addition, MtvS modulates transcription of many genes in stationary phase, some of which are required for *Francisella* virulence. Pull-down experiments revealed MtvS interacts with the β' subunit of the RNA polymerase and therefore may constitute a noncanonical alternative sigma factor involved in the regulation of the expression of CRISPR loci and other genes.

34 **Introduction**

35 CRISPR (Clustered regularly short interspaced palindromic repeats)-Cas (CRISPR associated
36 genes) systems protect bacteria and archaea against foreign nucleic acids such as phages and
37 genetic mobile elements[1,2]. CRISPR-Cas systems are adaptive immune systems that can store
38 memories of previous infections in the form of short invader-derived sequences that are
39 inserted in between the repeats of the CRISPR array during infection[3–5]. CRISPR arrays are
40 transcribed into CRISPR RNAs (crRNAs) that guide Cas effectors to complementary
41 sequences on the invading foreign genomes[6,7] to stop infection [8–13]. Prokaryotic organisms
42 often encode multiple CRISPR-Cas loci, which may be differently regulated[14]. Previous
43 studies have reported Cas proteins, crRNAs, transcriptional regulators, quorum sensing and
44 two component signaling systems involved in the regulation CRISPR-Cas systems [15–35].
45 Detailed investigation of regulatory networks governing CRISPR expression, however, has
46 been difficult due to the lack of natural hosts that can be used as experimental systems for
47 CRISPR-Cas immunity.

48 Here we studied the endogenous type II-B and type V-A CRISPR-Cas systems in the
49 opportunistic human pathogen *Francisella tularensis* subspecies *novicida* Utah 112 (here *F.*
50 *novicida* U112) (Fig. S1A-B)[13,36,37]. It has been shown previously that both *F. novicida*
51 systems are functional and capable of restricting foreign DNA[38,39]. Interestingly, *F. novicida*
52 Cas9 is also required for virulence and enhances membrane stability by repressing an operon
53 containing a lipoprotein with unknown function[40–43]. However, little is known about how
54 these two systems are transcriptionally controlled, especially in the light of the limited sets of
55 canonical regulatory proteins encoded by *Francisella*[44]. For example, *Francisella* possesses
56 only two canonical sigma factors (σ^{70} and σ^{32}) to dictate promoter specificity and initiation of
57 transcription[44,45]. *Francisella* also has a unique RNA polymerase that contains two
58 heterologous α subunits (instead of two identical subunits) which may also impact promoter
59 recognition[46–48].

60 Using fluorescence microscopy, we found that the two *F. novicida* CRISPR-Cas systems are
61 differentially regulated and expressed in non-infection conditions. While the type II-B
62 CRISPR-Cas system is constitutively expressed, the type V-A CRISPR-Cas system displays
63 significantly higher expression during stationary phase. Using mass spectrometry and genetics
64 we identified MtvS (Modulator of the type V-A CRISPR-Cas system expression in stationary
65 phase, FTN_1238), a protein with previously unknown function in *Francisella* species, as a
66 factor required for the differential expression of the type V-A CRISPR-Cas locus.

67 Additionally, we showed that type V-A CRISPR-Cas system expression is induced upon
68 introduction to spent overnight medium suggesting that *F. novicida* is capable of quorum
69 sensing despite lacking canonical quorum sensing genes. Last, we demonstrated with pull-
70 downs that MtvS interacts with the β' subunit of RNA polymerase. Since MtvS does not only
71 affect the expression of the type V-A CRISPR-Cas system but of several genes in stationary
72 phase, we hypothesize that MtvS may act as a noncanonical sigma factor.

73

74 **Results**

75 *The F. novicida Type V-A CRISPR-*Cas *locus is upregulated during stationary phase*

76 To investigate the expression pattern of the type II-B and type V-A CRISPR-Cas systems in
77 *F. novicida* U112, their RNA-guided nucleases were C-terminally tagged to generate Cas9-
78 msfGFP and Cas12-mCherry2, respectively. The fluorescent tags did not affect their nuclease
79 function, since plasmid interference assays confirmed that the tagged nucleases prevented
80 plasmid conjugation as well as the native ones (Fig. S1C). Fluorescence live-cell imaging of
81 exponentially growing bacteria and cells in stationary phase revealed that fluorescence
82 intensity was comparable in both growth phases for Cas9-msfGFP while fluorescent intensity
83 for Cas12-mCherry2 was higher in stationary phase (Fig. 1A). Relative quantification of
84 expressed proteins in the unlabeled parental strain revealed broad changes in protein
85 expression between exponential and stationary phase cells (Fig. 1B, Supplementary Data File,
86 tabs A-B). Gene set enrichment (GSE) analysis (Supplementary Data File, tab B) suggested
87 that proteins involved in DNA replication and cell envelope biogenesis were expressed at
88 significantly higher levels in exponential growing cells. On the other hand, DNA repair and
89 anti-stress proteins were more prominent in stationary phase cells. Furthermore, this
90 untargeted proteomics approach corroborated that Cas12 expression was increased about 1.8-
91 fold in stationary phase, and showed no phase variation for Cas9 (Fig. 1B, Supplementary
92 Data File, tab A). In addition to the two effector nucleases, only $Cas1_{type\ II\text{-}B}$ was detected in
93 the tested conditions (Supplementary Data File, tab A). To investigate whether these distinct
94 expression patterns of Cas9 and Cas12 originate from different transcription levels, we
95 performed RNA-seq. Similar to the proteomics data, comparison of RNA levels of genes
96 between exponentially growing and stationary phase bacteria revealed broad changes in gene
97 expression between the two growth conditions. Genes required for protein synthesis were
98 expressed higher in exponential phase growing cells and genes involved in metabolizing
99 different substrates were upregulated in stationary phase (Fig. 1C, Supplementary Data File,

100 tabs C-E). Importantly, *cas12* and *cas2*$_{type\ V\text{-}A}$ RNA levels were significantly higher during
101 stationary phase than in exponential growth phase (Fig. 1C, Supplementary Data File, tabs C-
102 D). In comparison, components from the type II-B CRISPR-Cas system, except *cas2*, had
103 comparable RNA levels in the two tested conditions (Fig. 1C, Supplementary Data File, tabs
104 C-D). Targeted measurement of RNA levels of *cas9* and *cas12* by RT-qPCR confirmed the
105 invariability of RNA levels of *cas9* in the two growth conditions and the distinct temporal
106 expression of *cas12* in stationary growth phase (Figs. 1D and 1E). Together these results
107 show that the two effector nucleases from the *Francisella* type II-B and type V-A CRISPR-
108 Cas systems have different expression patterns and that *cas12* expression levels significantly
109 increase in stationary phase.

110 *MtvS is required for upregulation of the Type V-A CRISPR-Cas locus in stationary phase*

111 Type V-A CRISPR-Cas systems have been shown to be autorepressed by Cas12 loaded with
112 *cas*-regulating RNAs[30]. Moreover, *F. novicida* U112 *cas12* promoter sequence contains a
113 predicted small repeat unit (SRU, with a similar but not identical sequence to the canonical
114 CRISPR repeat, Fig. S1B), which was proposed to have a regulatory function[29]. To test if
115 Cas12 is responsible for the upregulation of the type V-CRISPR-*Cas* locus we replaced *cas12*
116 with *mCherry2*. However, the fluorescence pattern did not change in absence of *cas12* (Fig.
117 2A). Next, we determined the exact transcription start site by 5' RACE to get a better
118 understanding of the promoter and its regulatory sequences. Interestingly, while we identified
119 a canonical -10 sequence (TATAAT), the putative -35 sequence is much less conserved
120 (AAGATT) (Fig. 2B). We then used this promoter sequence to perform *in vitro* transcription
121 assays with *E. coli* RNA polymerase holoenzyme. Using a fluorescence assay (see Methods),
122 we detected only basal levels of aptamer transcription with the *cas12* promoter, indicating that
123 it is not recognized by *E. coli* σ^{70} (Fig. 2C). In contrast, an aptamer with the *cas9* promoter
124 was transcribed (Fig. 2C). In conclusion, these results suggest that *Francisella cas12*
125 transcription requires additional, noncanonical factors.

126 To identify such factors, we performed a protein pull-down using as baits the *cas12* promoter
127 DNA sequence and an intragenic *cas12* sequence as a control. Lysates from exponentially
128 growing and stationary bacteria were probed and pull-down proteins were identified proteins
129 by LC-MS/MS. All identified proteins are listed in the Supplementary Data File, tabs F-G. An
130 enrichment score was calculated by comparing protein abundance in pull-downs from the
131 *cas12* promoter sequence to the control sequence. In exponentially growing cells, one of the
132 most significantly enriched proteins was the LysR-family transcriptional regulator FTN_0392

133 (Fig. 3A, Supplementary Data File, tab F). However, neither Cas12-mCherry2 expression nor
134 type V-A-mediated plasmid targeting was decreased in a *FTN_0392* deletion mutant (Fig.
135 S2A-B). On the other hand, in the stationary growth sample, FTN_1238 was significantly
136 enriched (Fig. 3B, Supplementary Data File, tab G). Importantly, there was no enrichment for
137 FTN_1238 when using a lysate from exponentially growing bacteria (Fig. 3A). *FTN_1238* is
138 the first gene of an operon encoding for genes required for the respiratory chain (*ubiH*, *ubiF*),
139 a putative phage protein (*FTN_1235*) and a tRNA modification enzyme (*queA*) (Fig. S2C).
140 FTN_1238 has no assigned function in *Francisella* yet but is homologous to YgfB (Fig. S2D),
141 which is conserved in many γ-proteobacteria[49].

142 To test if FTN_1238 was involved in regulation of *cas12* expression, we made a non-sense
143 mutation by introducing three stop codons after aspartate at position 11 and analyzed the
144 mutant cultures via fluorescence microscopy. We found decreased fluorescence of Cas12-
145 mCherry2 in stationary phase for this mutant and the phenotype could be rescued by
146 introducing a wild-type copy of *FTN_1238* with its native promoter at the Tn7 introduction
147 site downstream of gene *glmS* (*FTN_0485*) (Fig. 3C). Importantly, the *FTN_1238* nonsense
148 mutant and parental strain grew in a comparable manner, suggesting that the disruption of
149 FTN_1238 did not have pleiotropic effects (Fig, S2E). In contrast, disruption of FTN_1238
150 significantly affected the RNA levels of all type V-A CRISPR-Cas system genes in stationary
151 phase as measured by RT-qPCR (Fig. 3D-G). RNA levels were restored with an additional
152 wild-type copy of *FTN_1238* except for *cas2*, the last gene of the operon (Fig. 3D-G).
153 Interestingly, while the disruption of *FTN_1238* had a detrimental effect on *cas12* RNA levels
154 in stationary phase, the targeting capability of Cas12 in plasmid interference assays was not
155 affected (Fig. S2F). Moreover, despite being only enriched in the pull-down with the *cas12*
156 promoter and stationary phase lysate, *FTN_1238* RNA levels were comparable in both growth
157 phases (Fig. S2G, table 12). Fluorescence microscopy suggests slightly higher proteins levels
158 of FTN_1238-mCherry2 in stationary phase, however no increase of protein levels in
159 stationary phase was observed with LC-MS/MS (Fig. S2H, Supplementary Data File, tab A).
160 In summary, our results indicate that FTN_1238 is a modulator of the type V-A CRISPR-Cas
161 system expression in stationary phase, and therefore we renamed it MtvS.

162 *Quorum sensing signals participate in the regulation of the Type V-A CRISPR-*Cas *locus*

163 During stationary phase the cell density is high. Interestingly, microscopy of exponentially
164 growing cells in microfluidic plates showed that Cas12-mCherry2 is also expressed in a MtvS
165 dependent manner in this growing phase within densely populated areas (Fig. 4A-B, Movies 1

166 and 3), but not in less dense regions belonging to the same flow chamber (Fig. 4A-B, Movies
167 2-4). These results led us to hypothesize that quorum sensing signals, which are normally
168 secreted to the medium when bacterial cultures reach high density, could play a role in
169 regulating the type V-A CRISPR-Cas system. Therefore, we tested if the addition of spent
170 overnight medium could increase *cas12* expression in exponential cultures of *F. novicida*
171 U112. We replaced the medium of exponentially growing cells with spent overnight medium
172 filtered with 0.2 µm filters in microfluidic plates and monitored individual cells by
173 microscopy. We observed drastic changes, with bacteria changing from rod to coccus shapes,
174 and an increased Cas12-mCherry2 fluorescence (Fig. 4C, Movie 5). Fresh medium reversed
175 these changes and cells resumed growth as rod-shaped and Cas12-mCherry2 expression
176 decreased (Fig. 4D, Movie 5). Heat-treatment of the spent overnight medium eliminated its
177 activity on exponentially growing bacteria (Fig. S3A, Movie 6). When exposed to overnight
178 spent medium, *mtvS* nonsense mutant cultures also suffered rod-to-coccus shape changes, but
179 displayed much lower Cas12-mCherry fluorescent signal, indicating that Cas12-mCherry2
180 was less expressed (Fig. 4E-F, Movie 7). This result was confirmed by RT-qPCR, using RNA
181 extracted from parental strain and *mtvS* nonsense mutant cells before, 0.5 h and 1 h after
182 switching to spent overnight medium and probed for *cas12* and *cas9* RNA levels. While
183 *cas12* RNA levels increased over 1 h after the medium change, *cas9* RNA levels did not
184 significantly change (Fig. 4G and Fig. S3B). Together these results suggest that *F. novicida*
185 U112 may integrate quorum sensing signals into the MtvS dependent regulation of Cas12
186 expression.

187 *MtvS modulates expression of several genes in stationary phase*

188 To investigate if MtvS acts on more genes than only the type V-A operon, we performed
189 RNA-seq of the *mtvS* mutant, using RNA extracted from bacteria grown to exponential and
190 stationary phase (Supplementary Data File, tabs C-D). Comparison of RNA levels revealed
191 that expression of the type V-A CRISPR locus is comparable in both growth conditions in this
192 mutant confirming that MtvS is required for differential expression of this locus in stationary
193 phase (Fig. 5A, Supplementary Data File, tabs C-D). Intriguingly, principal component
194 analysis and clustering of genes with similar expression patterns revealed differences between
195 the parental strain and the *mtvS ns* mutant in particular in stationary phase samples (Fig. 5B,
196 S4A). In exponential phase, only a few genes with differential expression patterns between
197 the parental strain and teh *mtvS* mutant were observed (Supplementary Data File, tab C), GSE
198 analysis suggests that in the *mtvS* mutant, downregulated genes are involved in cell envelope
199 biogenesis and tRNA modification while genes involved in protein unfolding are upregulated

200 (Supplementary Data File, tabs C and E). Differences between the parental strain and the *mtvS*
201 mutant were more profound in stationary phase with more genes being significantly
202 differentially expressed (Supplementary Data File, tab C). Especially genes involved in
203 energy production and conversion as well as cell envelope biogenesis genes were affected
204 (Supplementary Data File, tabs C and E). Interestingly, many of these genes were affected
205 more severely than *cas12* (Supplementary Data File, tab C).

206 Analysis of promoter sequences of significantly downregulated operons (Supplementary Data
207 File, tab E) in both exponential and stationary phase in the *mtvS* mutant compared to the
208 parental strain revealed that 55 % of these promoters (34/62) encoded a TATAAT sequence
209 similar to the -10 element of the *cas12* promoter. In contrast, only 33 % of promoters (14/43)
210 of upregulated operons (Supplementary Data File, tab E) contained a TATAAT sequence. The
211 alignment of promoters of downregulated operons that encode a TATAAT sequence suggests
212 a putative -35 sequence starting with a highly conserved T (Fig. 5C). However, the *cas12*
213 promoter is one of the few examples which does not encode a T as first base pair in its
214 putative -35 element.

215 Absence of MtvS also led to changes in the proteome. Interestingly, Cas12 protein levels were
216 still higher in stationary phase, however the difference between the two growth phases was
217 less pronounced than for the parental strain (Fig. 5D, table 9). This result provides a possible
218 explanation for the high Cas12-dependent plasmid targeting levels detected for the *mtvS*
219 mutant strain (Fig. S2B). Some significant differences in protein expression between the
220 parental strain and the *mtvS* mutant were observed for both growth phases (Fig. 5E, S4B,
221 Supplementary Data File, tabs A-B). Most differences were observed for the exponential
222 growth phase with a decrease in the abundance of 30 proteins and an increase in the levels of
223 12 proteins in the *mtvS* mutant, when compared to the parental strain (Supplementary Data
224 File, tab A). Most of these proteins are involved in energy production and conversion
225 (Supplementary Data File, tab B). In stationary phase, fumarylacetoacetase (FTN_0910)
226 involved in phenylalanine and tyrosine degradation and RuvB (FTN_0891) involved in DNA
227 repair were less expressed while an acetyltransferase (FTN_1750) involved in
228 glycerophospholipid synthesis was expressed to higher levels in the *mtvS* mutant
229 (Supplementary Data File, tabs A-B). In summary, our results indicate that MtvS modulates
230 expression of several genes and its effects are most pronounced transcriptionally in stationary
231 phase.

232 *MtvS interacts with the β' subunit of RNA polymerase*

233 To investigate the mechanism by which MtvS modulates *cas12* transcription, we purified a
234 His_6-tagged version of the protein and tested whether it binds directly to the *cas12* promoter.
235 However, electrophoretic mobility shift assays indicated that his is not the case (data not
236 shown). This suggested that MtvS might interact indirectly with DNA, possibly through
237 interactions with another protein. Therefore, we used the purified His_6-MtvS as bait to pull
238 down potential partners from lysates of *mtvS* mutant cells grown to stationary phase.
239 Importantly, a strain encoding *mtvS-His$_6$* on the chromosome and the parental strain had
240 comparable *cas12* RNA levels suggesting that the His_6-tag did not alter MtvS' function (Fig.
241 S5A). In addition, both MtvS-His_6 purified from *E. coli* and chromosomal MtvS-His_6 in *F.*
242 *novicida* U112 possessed a similar molecular weight that ran slightly lower on SDS-PAGE
243 gels than predicted (calculated molecular weight including His_6-tag: 20.9 kDa) (Fig. S5B-C).
244 LC-MS/MS analysis of the pull-down with MtvS-His_6 revealed that two DNA-binding
245 proteins and a putative anti-anti sigma factor were among the significantly enriched proteins
246 (Fig. 6A, Supplementary Data File, tab H). However, while deletion of *FTN_0565* (containing
247 a Lambda repressor-like DNA binding domain) was not possible in our hands, deletion of
248 *FTN_ 0324* (putative anti-anti sigma factor with STAS domain) and *FTN_1282* (LysR family
249 transcriptional regulator) did not affect Cas12-mCherry2 expression (Fig. S5D).

250 Another protein that was significantly enriched in the pull-down was RpoC (FTN_1567), the
251 β' subunit of RNA polymerase (Fig. 6A, Supplementary Data File, tab H). To probe for an
252 interaction between MtvS and RNA polymerase (RNAP), a pull-down with purified MtvS-
253 His_6 and commercially available *E. coli* RNAP core enzyme and holoenzyme (RNAP core
254 enzyme in complex with σ^{70}) was performed. We found that *E. coli* RNAP core enzyme was
255 pulled down with MtvS-His_6 regardless of whether σ^{70} was present or not (Fig. 6B). To
256 understand how MtvS possibly interacts with the RNA polymerase, we modelled *Francisella*
257 RNAP core enzyme together with MtvS in AlphaFold 3 (Fig. 6C, S5E)[50]. Intriguingly,
258 AlphaFold 3 confidently predicted that MtvS primarily binds the coiled-coil domain of the β'
259 subunit similar to σ^{70} (domain 2) and σ^{32} (Fig. 6C, S5E)[51,52]. A list of these predicted
260 interactions between RpoC and MtvS can be found in table 7. Importantly, the β' coiled-coil
261 domain is predicted to dock into a pocket of MtvS similar to what was found for σ^{70} (Fig. 6D,
262 S5F)[53]. This pocket among other regions also contains several residues conserved between
263 MtvS and *E. coli* homolog YgfB possibly explaining why MtvS can interact with *E. coli* RNA
264 polymerase (Fig. S5G). In conclusion, our results show that MtvS binds to the β' subunit of
265 RNAP likely at the β' coiled-coil domain. This would suggest that the binding of MtvS and
266 the two known sigma factors of *Francisella* to RNAP are probably mutually exclusive. This

267 may also explain why the RNA polymerase holoenzyme was pulled down to a lesser extent
268 than the core enzyme (Fig. 6B).

269 Since MtvS likely binds the same β' coiled-coil domain as the 2.2 region of σ^{70} and modulates
270 expression of several genes, we hypothesized that MtvS may be a noncanonical alternative
271 sigma factor similar to the smaller extracytoplasmic function (ECF) and phage sigma
272 factors[54–56]. Because domain 2 of σ^{70} is also involved in recognition and melting of the -10
273 promoter element[57] it is possible that MtvS has a similar role. However, MtvS alone nor
274 together with σ^{70} did not promote transcription of the *cas12* promoter (Fig. 6F).

275 **Discussion**

276 Here we compared the expression of the two native type II-B and type V-A CRISPR-Cas
277 systems in *F. novicida* U112 in the absence of phage infection. We found that while the type
278 II-B CRISPR-Cas system is continuously expressed throughout growth in liquid culture, the
279 type V-A CRISPR-Cas system is significantly upregulated at high cell density and stationary
280 growth phase. We envision different possibilities behind this unique regulation. First, it is
281 known that bacteria enhance their anti-phage defenses in high cell density environments when
282 they are more vulnerable to phage predation[15,16,58–64]. Given that the type II-B system is
283 constitutively expressed, the upregulation of the type V-A system will equip *F. novicida* U112
284 with additional defenses in stationary phase. It is also possible that Cas12 or other
285 components of the type V-A CRISPR-Cas system have a role beyond immunity in stationary
286 growth phase, analogous to the function of *F. novicida* Cas9 in the regulation of lipoprotein
287 expression[40–43]. Our proteomics and RNA-seq experiments showed drastic changes in
288 transcription and translation in stationary phase, indicating the need to adapt to this growth
289 condition, an adaptation in which Cas12 could play a part that would justify its upregulation
290 in this growth phase.

291 We identified MtvS, a protein with previously unknown function in *F. novicida* U112, as a
292 factor required for the transcriptional upregulation of the type V-A CRISPR-*cas* lucus in
293 stationary phase and upon addition of spent overnight medium to the exponentially growing
294 cultures (Fig. 3 and 4). MtvS belongs to the YecA/YgfB-like protein family and is conserved
295 in many γ-proteobacteria[49]. Besides the structure of *Haemophilus influenzae* YgfB, little is
296 known about the function of this family of proteins[65]. In *Pseudomonas aeruginosa*, YgfB
297 increases β-lactam resistance through interactions with the antitermination factor AlpA that
298 lead to the upregulation of AmpC expression[66,67]. We believe that it is unlikely that MtvS
299 interacts with an anti-termination factor in *F. novicida* U112 since *cas12* transcription

300 decreases in the *mtvS* mutant (Fig. 3). Most importantly, we found that MtvS interacts with
301 the β' subunit of RNA polymerase in *Francisella* (Fig. 6). Intriguingly, MtvS is predicted to
302 bind the similar coiled coil domain of the β' subunit as σ^{70} (domain 2) and σ^{32} [51,53,68,69].
303 Domain 2 of σ^{70} is required for recognition and melting of the -10 promoter sequence [57].
304 Since *Francisella* only possesses two sigma factors[44], σ^{70} and σ^{32}, it is tempting to speculate
305 that MtvS has a similar role. The broad transcriptional changes, especially in stationary phase,
306 caused by the disruption of MtvS seem to support this hypothesis (Fig. 5). An analysis of
307 promoters of the downregulated operons in stationary phase in the *mtvS* mutant showed that
308 more than half of these promoters encode the same -10 sequence as the *cas12* promoter
309 (TATAAT). While it is possible that these genes that are directly regulated by MtvS, it is also
310 possible that they are up- or downregulated as part of a compensatory mechanism that takes
311 place in the absence of MtvS.

312 Although we hypothesize that MtvS may act as a noncanonical sigma factor, MtvS alone nor
313 together with σ^{70} is sufficient to promote transcription of the *cas12* promoter *in vitro*. We
314 noticed that MtvS is too small to fulfill the role of domain 4 of σ^{70}, which interacts with the β-
315 flap and recognizes the -35 promoter sequence[51,70]. Therefore, one possibility is MtvS might
316 be part of a split sigma factor together with a yet unidentified protein similar to Gp55 and
317 Gp33 in T4 phage. Gp55 and Gp33 together with the DNA clamp Gp45 initiate transcription
318 of late T4 genes by taking over the roles of domain 2 and domain 4 of σ^{70} , respectively[71–73]. It
319 is also possible that MtvS indirectly modulates gene transcription through one of the
320 canonical sigma factors. This is unlikely because first, in contrast to the *cas9* promoter, σ^{70}
321 does not lead to initiation of transcription of the *cas12* promoter in our *in vitro* transcription
322 assays and second, the *cas12* promoter does not contain a canonical σ^{32} motif[74]. Most
323 importantly, none of the sigma factors were significantly enriched in the MtvS-His_6 pull-down
324 (Fig. 6).

325 Last, *F. novicida* U112 cells reacted strongly to spent overnight medium, displaying a growth
326 arrest, morphological changes and an increase in Cas12 expression, the latter also dependent
327 on the presence of MtvS. Changes in gene expression as reaction to spent overnight medium
328 is a hallmark of quorum sensing[75]. Intriguingly, *F. novicida* U112 lacks canonical quorum
329 sensing genes[76]. Our results suggest that the type V-A CRISPR-Cas system and MtvS could
330 be part of a yet to be described quorum sensing circuit that monitors and responds to changes
331 in cell density. Future studies will investigate the quorum sensing network and the exact
332 mechanisms of how MtvS promotes transcription of *cas12* and other genes, relevant not only
333 for the understanding phage defense strategies but also for the pathogenesis of *Francisella*.

334 Since MtvS homologs are conserved, it will be also interesting to elucidate their roles in other
335 bacterial species as well.

Author Contributions. M.B. and L.A.M. conceived the study. C.F.B. carried out the MtvS-His_6 purification. J.C. expressed and purified the *E. coli* RNAP core enzyme and σ^{70} factor. E.A.C analyzed data and contributed to figures. M.B. performed all the other experiments. M.B. and L.A.M. wrote the manuscript with the help of E.A.C. All authors read and approved the manuscript.

Acknowledgments. We thank D.M. Monack (Stanford University) for the conjugation plasmid pDMK3, A. Harms (ETH Zurich) and C. Dehio (Biozentrum, University of Basel) for the *E. coli* conjugation strain, M. Basler (Biozentrum, University of Basel) for plasmid pFNMB2 *msfGFP*, H. Molina and C. Peralta (Proteomics Resource Center, The Rockefeller University) for performing and analyzing the LC-MS/MS experiment. Proteomics data was generated by the Proteomics Resource Center at The Rockefeller University (RRID:SCR_017797) using instrumentation funded by the Sohn Conferences Foundation and the Leona M. and Harry B. Helmsley Charitable Trust. We thank M. Lilic from the Campbell lab for advice on transcription assays. Thanks also go all members of the Marraffini lab (The Rockefeller University) for scientific discussions and feedback. M.B. was supported by the SNSF Early Postdoc.Mobility (P2BSP3_195673) and SNSF Postdoc.Mobility (P500PB_210998) fellowships. E.A.C is supported by the Rockefeller University and R35 GM151879. L.A.M. is an investigator of the Howard Hughes Medical Institute.

Competing interests. LAM is a cofounder and Scientific Advisory Board member of Intellia Therapeutics, a cofounder of Eligo Biosciences and a Scientific Advisory Board member of Ancilia Biosciences.

357 **Material and Methods**

358 **Bacterial strains and growth conditions**

359 *Francisella novicida* U112 (*F. novicida* U112) and associated mutants were grown
360 aerobically in brain heart infection (BHI, BD Biosciences) broth or on BHI agar plates
361 supplemented with 0.1 % L-cysteine (Sigma Alderich) and 50 µg/ml ampicillin (GoldBio). F.
362 *novicida* strains carrying plasmids were grown with 15 µg/ml kanamycin (GoldBio).

363 To receive exponentially growing cultures, stationary phase cells were diluted 1:20 in fresh
364 media and grown for 2-3 h until they reached an OD_{600} of 0.5-0.8 and had a rod-shaped
365 morphology. Stationary phase cells were grown over night for at least 16 hours until they
366 reached an OD_{600} of 3.5-4.5 and displayed a more coccus-like cell shape. Cell morphology
367 was checked by microscopy.

368 *Escherichia coli* OneShotpir (*E. coli,* Thermo Fisher Scientific) and derivative strains were
369 aerobically grown in Luria broth (LB, BD Biosciences) or on LB agar plates supplemented
370 with 50 µg/ml kanamycin at 37 °C. For conjugation *E. coli* JKE201 1.2 mM 2,6-
371 Diaminopimelic acid (DAP, Sigma Alderich) was added to all growth media since this strain
372 is auxotrophic for mDAP.

373 *E. coli* Rosetta 2 (DE3) (Novagen) containing the pET21 overexpression plasmid was grown
374 aerobically in LB with 100 µg/ml ampicillin.

375 *E. coli* BL21 (DE3) (Novagen) containing the pVS11 and pACYC-Duet1_*EcoRpoZ*
376 expression plasmid was grown aerobically in LB with 100 µg/ml ampicillin and 34 µg/ml
377 chloramphenicol (GoldBio) to overexpress *E. coli* RNAP core enzyme.

378 *E. coli* BL21 (DE3) containing the pSAD1403 expression plasmid was grown aerobically in
379 LB with 50 µg/ml kanamycin to overexpress *E. coli* σ^{70} factor.

380 Strains used for this study are listed in table 1.

381

382 **Bacterial mutagenesis**

383 To generate chromosomal in-frame *F. novicida* U112 mutants, suicide vector pDMK3 was
384 used [77]. For fluorescent tags, an Ala-Ala-Ala-Gly-Gly-Gly linker was added and after the stop
385 codon the 30 bp sequence of the gene was repeated to avoid downstream polar effects. For the
386 His-tags only a Gly linker was added. In-frame deletions yielded in peptide scars containing
387 the first and last 10 amino acids. Mutagenesis and conjugation was carried out as reported
388 previously [78,79]. For conjugation, donor *E. coli* JKE201 from A. Harms and C. Dehio [80] and
389 recipient *F. novicida* strains were grown until a OD_{600} of 1 was reached. 1 ml of each culture
390 was mixed in 20 µl of LB and spotted on a LB agar plate supplemented with 1.2 mM DAP
391 and incubated over night at 25 °C. The mixture was plated on Mueller Hinton (BD
392 Biosciences) agar plates supplemented with 0.1 % L-cysteine, 0.1 % D-glucose (Sigma
393 Alderich), 0.1 % heat inactivated fetal calf serum (Gibco), 50 µg/ml ampicillin and 15 µg/ml
394 kanamycin and incubated at 37 °C for 2 days. *F. novicida* colonies containing the suicide
395 vector were restreaked on BHI agar plates supplemented with 15 µg/ml kanamycin. To select
396 against pDMK3, individual colonies were restreaked on LB agar plates supplemented with 5
397 % sucrose (Sigma Alderich), 0.1 % L-cysteine and 50 µg/ml ampicillin and incubated at 25
398 °C until colonies lost the suicide vector. Each mutant was verified by colony PCR using
399 primers binding outside of the recombined region and sequencing of these regions. In
400 addition, they were restreaked on kanamycin again to check for loss of pDMK3.

401 All primers and plasmids are listed in table 2.

402

403 **Fluorescence live cell imaging**

404 A Nikon Ti-E inverted motorized microscope equipped with Perfect Focus System and a CFI
405 Plan Apochromat DM Lambda 100X Oil objective lens (NA 1.4) was used for live-cell
406 imaging. A SOLA Light Engine (Lumencor) set to 5 % power and C-FL GFP HC HISN Zero
407 Shift filter (excitation: 470/40 nm (450–490 nm), emission: 525/50 nm (500–550 nm),
408 dichroic mirror: 495 nm) and C-FL DS RED HC HISN Zero Shift filters (excitation:
409 545/30nm (530-560nm), emission: 620/60nm (590-630nm), dichroic mirror: 570nm),
410 respectively, were used to excite and filter fluorescence from msfGFP and mCherry2. The
411 exposure time for each channel was set to 500 ms and images were collected with a Zyla 4.2
412 sCMOS (Andor, pixel size 65 nm) or an ORCA-FusionBT sCMOS camera (Hamamatsu,
413 pixel size 65 nm). Phase contrast was imaged with the SOLA light Engine set to 2% power
414 and 10 ms excitation. The microscope was controlled by the software NIS-Elements AR
415 version 5.21.03.

416 Exponentially grown (rod-shaped) and stationary phase (roundish) *F. novicida* were spun
417 down and resuspended in phosphate saline buffer (PBS, Gibco) and spotted on pads
418 consisting of 1% agarose in PBS. Snapshots of phase contrast, RFP and GFP channels were
419 taken immediately after.

420 Long-term imaging experiments which include switching of media were carried out in
421 CellASIC ONIX microfluidic plates (Millipore). Exponentially growing bacteria were
422 resuspended in BHI supplemented with 0.2 % L-cysteine and loaded into the microfluidic
423 plate along with fresh BHI supplemented with 0.2 % L-cysteine for initial growth and the
424 tested medium as specified in the Fig. legend. For generating spent overnight medium, cells in
425 stationary phase were pelleted for 1.5 minutes at 16000 g and supernatant was filtered with
426 0.22 µm filters (Millipore). For heat-treated spent overnight medium, filtered spent overnight
427 medium was incubated at 95 °C for 10-20 minutes. After connecting the plate to the CellASIC
428 ONIX2 Microfluidic System, the plates were incubated at 37 °C for 1 h using a Tokai HIT
429 thermal box (Zeiss). Images of phase contrast, RFP and GFP channel were taken every 5
430 minutes after loading cells into the imaging chamber. First, fresh BHI was flown over for 1 h
431 before switching to the tested medium for 4h. Afterwards, fresh BHI was flown over again for
432 3 h. For all media, the flow rate was set to 13.8 kPa.

433

434 **Image analysis**

435 Image analysis was carried out with Fiji software [81]. For comparison of fluorescent signal
436 intensities, the contrast was set to same values for sets of compared images in same sub panel.
437 If compared across sub panels, it is stated in Fig. legend which contrasts are set to same
438 values.

439 For long-term imaging, images were aligned to the first image using NIS-Elements AR
440 version 5.21.03.

441

442 **RNA-seq**

443 RNA was extracted from exponentially growing and stationary phase cells in three biological
444 replicates for each condition. Cells yielding in a total OD_{600} of 3 were pelleted and
445 resuspended in 80 µl of PBS and 20 µl of 10 % Sarcosyl (Sigma Alderich). Then, RNA was
446 extracted with TRI Reagent according to the manufacturer's protocol (Zymo Research). An
447 in-column DNA digest during RNA extraction was performed. A second DNA digestion was
448 carried out with 10 µg of RNA using Turbo DNase (Invitrogen) for 2x 30 minutes. The DNA-
449 free RNA was cleaned up with the RNA Clean & Concentrator-5 kit (Zymo Research) and

450 eluted in 15 µl of water. RNA quality was checked by running a bleach agarose gel[82]. RNA
451 concentrations were measured with a Qubit 4 fluorometer (Invitrogen) using the Qubit RNA
452 Broad Range Assay Kit.

453 Ribosomal RNA was depleted with the NEBNext rRNA depletion (bacteria) kit (NEB). An
454 input of 1 µg of RNA was used. Then, the RNA was prepared for sequencing using the
455 TruSeq Stranded mRNA kit (Illumina) according to manufacturer's instruction. For the first
456 strand synthesis, Superscript IV reverse transcriptase (Invitrogen) was used with an annealing
457 temperature of 50 °C. Final DNA concentrations and lengths were measured with a Qubit 4
458 fluorometer (Invitrogen) using the Qubit dsDNA High Sensitivity Assay Kit and the
459 Tapestation 4200 bioanalyzer (Agilent) with the Agilent D500 ScreenTape Assay (Agilent).

460 The DNA libraries were diluted to 12 pM and mixed with 2.5% 20 pM PhiX and subjected to
461 single read sequencing with a 150-cycle MiSeq Reagent Kit v3 (Illumina) on the Illumina
462 MiSeq platform.

463 The reads were mapped to the *F. novicida* U112 genome (RefSeq NC_008601[83]) and RPKM
464 values for each gene was calculated using coordinates of coding genes (ptt files) and of
465 rRNAs and tRNAs (rtt files) with EDGE-Pro v1.3.1[84]. EDGE-Pro statistics for each sample
466 can be found in table 3. Significant changes in gene expression between used conditions were
467 calculated with the R (version 4.3.0) package DESeq2 (version 1.40.2)[85]. Results and
468 normalized counts are listed in tables 12-13. rRNAs (*FTN_0472, FTN_0475, FTN_0476,*
469 *FTN_0501, FTN_1304, FTN_1305, FTN_1308, FTN_1720, FTN_1721, FTN_1724*) are
470 marked in italic in the table and excluded in the graphs. *P*-values of 0.05 (Wald test) or
471 adjusted *p*-value (Benjamini-Hochberg) of 0.05 and log2 foldchanges of 2 were defined as
472 significant.

473

474 **RT-qPCR**

475 RNA was extracted as reported for RNA-seq. The RNA was reverse transcribed to cDNA
476 with Superscript IV reverse transcriptase (Invitrogen) using 1 µg of RNA, random hexamer
477 primers, and a reaction temperature of 50 °C.

478 qPCR was performed in the QuantStudio 3 Real-Time PCR System (Applied Biosystems)
479 using the PowerUp SYBR Green Master Mix (Applied Biosystems). Reactions were set up in
480 a total volume of 20 µl containing 50 ng of cDNA template and 500 nM primers. Each
481 reaction was set up in three technical replicates. All primers used for RT-qPCR are found in
482 table 4. The annealing and amplification temperature was set to 60 °C.

483 The geometrical mean of the three technical replicates for each biological replicate was used
484 for further analysis. RNA levels of probed genes were normalized to the DNA 3'-5' helicase
485 gene *uvrD* (FTN_1594), which has been used previously for normalization and does not
486 change its expression in the used conditions as determined by RNA-seq[86]. The average value
487 of the three biological *uvrD* replicates was used to the ΔCt value for each gene. Relative RNA
488 abundance of probed genes was calculated as $2^{-\Delta Ct}$.

489 Statistical analysis for RT-qPCR data was performed with Prism10.2.3 (403) (GraphPad
490 Software). To test if relative RNA abundances determined by RT-qPCR are significantly
491 different, two-way ANOVA (α=0.05) with correction for multiple comparison (Tukey's
492 multiple comparisons test) was performed. Adjusted *p*-values are given in the figure. legends.

493

494 **5' RACE**

495 Rapid amplification of 5' cDNA ends (5' RACE) was carried out with RNA extracted as
496 reported for RNA-seq. Parental strain RNA from both growth phases in three biological
497 replicates was used. Sequences of template switch oligo (TSO) and primers are listed in table
498 5.

499 The manufacturer's protocol was followed. In short, 1 µg of RNA was annealed with the RT
500 primer for the gene of interest (10 µM) and 10 mM dNTPs (Thermo Fisher Scientific in a 6 µl
501 reaction at 70 °C for 5 minutes. Afterwards, the reaction was put on ice. Then the Template
502 Switching RT Enzyme Mix (NEB) and the template switch oligo (3.75 µM) were added (final
503 volume: 10 µl) and reverse transcription and template switching was performed in a
504 thermocycler (BioRad) for 90 minutes at 42 °C, followed by 5 minutes at 85 °C and hold at 4
505 °C. The reaction was diluted 1:2 with H2O. The 5' region of transcripts was amplified with a
506 touch down PCR using Q5 Hot Start High-Fidelity polymerase (NEB), 4 µl of the diluted
507 template and primers (10 µM) binding to the template switch oligo and to the gene of interest.

508

509 **Whole cell lysate proteomics**

510 Three biological replicates of exponentially growing and stationary phase parental strain cells
511 yielding a total OD_{600} of 5 were washed once with PBS and resuspended in 500 µl lysis byffer
512 (20 mM Tris-HCl pH 7.5, 100 ml KCl, 2 % NP-40 (Thermo Fisher Scientific), mini cOmplete
513 EDTA-free protease inhibitor cocktail). Samples were lysed by 4 rounds of sonication on ice
514 (40 % amplitude, 5 s pulses, 30 s breaks, Q500 sonicator). Cell debris was removed by
515 centrifugation at 21000 g, 4 °C for 10 minutes. Protein concentrations were measured with a
516 BCA protein assay (Pierce). Samples were stored at -80 °C until 50 µg of protein per sample
517 was subjected to LC-MS/MS analysis.

518

519 **Promoter sequence pull-down**

520 Pulldown of proteins binding the *cas12* promoter and the intragenic *cas12* control sequence
521 was carried out in three biological replicates as reported previously[87,88].

522 In short, primers with a 5' Biotin-TEG label were used to generate bait DNA sequences (table
523 6) from *F. novicida* gDNA. PCR products were checked by agarose gel and cleaned up with
524 QIAquick PCR Purification Kit (QIAGEN) and concentrated with Amicon Ultra-0.5 mL
525 Centrifugal Filters (Millipore Sigma) to 200 ng/µl in water. Washed Dynabeads MyOne
526 Streptavidin C1 (Invitrogen) were loaded with 40 µg of DNA for 20 minutes. DNA
527 concentrations in the removed supernatants were measured to ensure that most DNA bound to
528 the Dynabeads. Exponentially growing and stationary phase parental strain cells yielding a
529 total OD_{600} of 800 were resuspended in 5 ml 1x FastBreak cell lysis buffer (Promega) in
530 BS/THES buffer (10 mM HEPES (Thermo Fisher Scientific) pH 7.5, 5 mM $CaCl_2$
531 (Sigma_Aldrich), 50 mM KCl (Sigma-Aldrich), 12 % glycerol (Sigma-Aldrich), 22 mM Tris-
532 HCl pH 7.5 (VWR, Thermo Fisher Scientific), 4 mM EDTA (Thermo Fisher Scientific), 9 %
533 sucrose (Sigma-Aldrich), 62 mM NaCl (Sigma-Aldrich), mini cOmplete EDTA-free protease
534 inhibitor cocktail (Roche)) for 30 minutes on ice and then sonicated afterwards. 200 µl of
535 precleared lysates was added to the resuspended beads supplemented with 0.03 µg/µl salmon
536 sperm DNA (Thermo Fisher Scientific) and incubated for 1 h with agitation. The beads were
537 washed 5x with BS/THES buffer and 2x with wash buffer (100 mM NaCl, 25 mM Tris-HCl
538 pH 7.5 and then switched to new tubes before a last wash. The dried beads were stored at 4 °C
539 until they were subjected to LC-MS/MS analysis.

540 **MtvS-His pull-down**

541 Pull-down of proteins binding MtvS-His_6 was carried out by following the same protocol as
542 reported previously and used for the promoter sequence pull-down with changes indicated
543 below[87,88].

544 The *mtvS* nonsense mutant was grown to exponential and stationary phase in three biological
545 replicates yielding a total OD_{600} of 450 each and resuspended in 5 ml 1x FastBreak cell lysis
546 buffer in BS/THES supplemented with 0.5 mg/ml lysozyme (Sigma-Aldrich) and 0.1 mg/ml
547 DNase I (Roche). Lysis buffer did not contain EDTA as it is not compatible with the
548 Dynabeads His-Tag Isolation and Pulldown beads (Invitrogen) according to the manual. For
549 cell lysis, the samples were incubated shaking at 4 °C for 1 h and subsequently sonicated
550 according to promoter sequence pull-down protocol. Cell debris was removed by
551 centrifugation and filtration of lysates through 0.45 µm filters (Cytiva). 50 µl of prewashed
552 Dynabeads His-Tag Isolation and Pulldown beads per sample were loaded with 80 µg purified
553 MtvS-His_6 according to instructions and incubated on a roller at 4 °C for 30 minutes. Empty
554 beads subjected to the same treatment as beads loaded with MtvS-His_6 served as controls for
555 non-specific binders. After three washes, 350 µl lysates and 350 µl BS/THES buffer were
556 added to the beads and incubated on a roller at 4 °C for 1 h. Beads were washed similarly to
557 promoter pull-down protocol and the dried beads were stored at -20 °C until subjected to LC-
558 MS/MS analysis.

559

560 **LC-MS/MS analysis**

561 For whole cell lysates, proteins were reduced and alkylated followed by acetone precipitation.
562 Precipitates were dissolved in 50 µl 1 µg of trypsin (Promega)/60 mM ammonium
563 bicarbonate and digested overnight. An additional 1 µg of trypsin was added following
564 heating to 45 °C. Digestions were halted by adding 10% trifluoroacetic acid, volumes were
565 spun (16,000 g) and two thirds of the samples were subjected to solid phase extraction
566 (Empore). Data was acquired on an Ascend orbitrap mass spectrometer using either DDA or
567 DIA, and peptides were separated using a 25 cm EasySprayer column. A 120 minutes and 90
568 minutes analytical gradient increasing from 1% B to 30% B (B: 80% ACN,0.1% formic acid)
569 was used.

570 For the promoter sequence and MtvS-His_6 pull-downs, beads were resuspended in 8 M urea
571 and proteins were reduced and alkylated on beads. The supernatants were extracted, and
572 proteins were digested with LysC (Wako/Fuji) with urea concentration lowered to less than 4
573 M, followed by trypsination (Promega) with urea concentration lowered to less than 2 M.
574 Digestion was stopped with 10 % trifluoroacetic acid. Generated peptides were desalted and
575 concentrated with solid-phase extraction prior to analysis by LC-MS/MS (promoter sequence
576 pull-down: 12 cm packed-in-emitter column, 70 minutes analytical gradient, high
577 resolution/high mass accuracy mode (Dionex 3000 and Q-Exactive HF, Thermo Fisher
578 Scientific), MtvS-His_6 pull-down: 25 cm EASYSprayer column, 70 minutes analytical
579 gradient, high resolution/ high mass accuracy mode (Ascend)).

580 For analysis, generated data was searched and quantified using ProteomeDiscoverer (v
581 1.4.1.14 and 3.2)/Mascot (v 2.8 and 3.1), MaxQuant (v 2.0.3.0 and 2.6.6.0) and Spectronault
582 (v 19.7) and queried against Uniprot database for *F. tularensis* subspecies *novicida* U112
583 (taxon ID: 401614) concatenated with common contaminants to generate iBAQ values.
584 Statistical analysis was carried out with Perseus software (v 1.6.15.0). The values were log2
585 transformed and contaminants and proteins that have been identified in less than two
586 biological replicates of a sample were removed. After filtering, the data was median
587 normalized and normalized iBAQ values were produced.

588 For whole lysate proteomes, the values were log2 transformed and contaminants and proteins
589 that have not been detected in all three replicates for a least one condition were removed.
590 Missing values were imputed. Log2 foldchanges were calculated for each strain and
591 condition. An FDR-based (FDR = 0.05) two-sample t-test was used to determine which
592 changes were significant. Results are listed in table 9. *P*-values of 0.05 or adj*p*-values of 0.05
593 and log2 foldchanges of 1 were defined as significant.

594 For the pull downs, the values were log2 transformed and contaminants and proteins that have
595 been identified in less than two biological replicates of a sample were removed. After
596 filtering, the data was median normalized and normalized iBAQ values were produced. he
597 Log2 foldchange was calculated between proteins pulled-down with the *cas12* promoter
598 sequence and proteins pulled-down with the intragenic *cas12* control sequence for both
599 exponential and stationary conditions. An FDR-based (FDR = 0.05) two-sample t-test was
600 used to determine which changes were significant. Results are listed in tables 16-18. *P*-values
601 of 0.05 or adj*p*-values of 0.05 and log2 foldchanges of 2 were defined as significant.

602

603 **Plasmid interference assay**

604 Strains were generated with the native Type II-B or Type V-A CRISPR array replaced by a
605 targeting or non-targeting spacer matching expression plasmid pFNMB2 *msfGFP*. These
606 strains were grown exponentially together with the donor *E. col*i strain harboring pFNMB2
607 *msfGFP*. Cells yielding a total OD_{600} of 1 were pelleted and washed once with LB. Then,
608 recipient *F. novicida* strains were mixed with donor *E. coli* in a final volume of 20 µl LB and
609 spotted on nitrocellulose filter membranes with a 0.22 µm pore size (Millipore) located on LB
610 agar plates supplemented with 1.2 mM DAP. The plates were incubated for 2 h at 37 °C
611 before the bacteria were resuspended in a final volume of 100 µl MH broth (BD Biosciences).
612 Serial dilutions in MH broth were carried out and 5 µl of each dilution was spotted in
613 technical duplicates on MH agar plates supplemented with 50 µg/ml ampicillin for calculation
614 of total number of colony forming units (CFUs) and on MH agar plates supplemented with 50
615 µg/ml ampicillin and 15 µg/ml kanamycin for calculation of transformants. The average
616 number of CFUs of the two technical replicates was used for calculating CFU/ml. Three
617 biological replicates for each strain were analyzed.

618

619 **Growth curves**

620 Strains were grown overnight in liquid cultures, diluted 1:20 the next day and grown until
621 OD_{600} of ~1. For OD_{600} measurements with a plate reader (Agilent Synergy H1), OD_{600} was
622 adjusted to 0.2 and cells were seeded in 150 µl per well in a 96-well plate (Greiner Cellstar,
623 flat bottom with lid) in technical triplicates. Absorbance at 600 nm was measured every 10
624 minutes for 24 h while plate was incubated at 37 °C and shaking with 567 cpm (3 mm).
625 Growth curves for three biological replicates per strain were measured. Means with standard
626 deviation are shown.

627

628 **SDS-PAGE**

629 For protein analysis by SDS-PAGE, 4-20 % polyacrylamide gels (BioRad) were used and
630 staining was performed with Coomassie Brilliant Blue R-250 (Biorad) in not indicated
631 otherwise.

632

633 **Western blot**

634 A *F. novicida* U112 strain encoding mtvS-His_6 on the chromosome was grown exponentially
635 and to stationary phase yielding a total OD_{600} of 200 and resuspended in 30 ml lysis buffer (50
636 mM HEPES pH 7.5, 250 mM NaCl, 10 % glycerol, 0.5 mg/ml lysozyme, 1 mM Tris (2-
637 Carboxyethyl) phosphine hydrochloride (GoldBio), mini cOmplete EDTA-free protease
638 inhibitor cocktail). The cells were lysed for 1 h at 4 °C shaking and sonicated for 15 rounds
639 on ice ice (70 % amplitude, 10 s pulses, 30 s breaks). 15 µl of samples were run on a SDS-
640 PAGE gel and then transferred to nitrocellulose membrane (0.2 µm, BioRad) using a Trans-
641 Blot Turbo transfer system (BioRad). After blocking the membrane in 5 % milk in TBST
642 (PBS, 0.05 % Tween 20 (Sigma-Aldrich)) for 1 h, MtvS-His_6 was probed with primary mouse
643 THE His Tag anti-His_6 antibody (GenScript, A00186) diluted 1:4000 in PBST at 4 °C
644 overnight. The membrane was incubated with the secondary goat anti-mouse IgG (H+L) HRP
645 antibody (Thermo Fisher Scientific, 31430) diluted 1:10000 in PBST for 1 h. HRP signal was
646 detected with Clarity Western ECL substrate (BioRad) and ImageQuant 800 (Amersham) in
647 SNOW imaging mode.

648

649 **Expression and purification of *E. coli* RNA polymerase**

650 Plasmid pVS11 (also called pEcrpoABC(-XH)Z) was used to overexpress each subunit of
651 RNA polymerase (full-length α, β, ω) as well as β'-PPX-His_{10} (PPX; PreScission protease site,
652 LEVLFQGP, GE Healthcare), and co-transformed with a pACYCDuet-1 plasmid containing
653 *E. col rpoZ* into *E. coli* BL21(DE3) to ensure saturation of all RNA polymerases with *E. coli*
654 RpoZ. The cells were grown in the presence of 100µg/mL ampicillin and 34µg/mL
655 chloramphenicol to an OD_{600} of 0.6 in a 37 °C shaker. Protein expression was induced with
656 1mM IPTG (final concentration) for 4h at 30 °C. Cells were harvested by centrifugation and
657 resuspended in 50mM Tris-HCl pH 8.0, 5% w/v glycerol, 10mM DTT, 1mM PMSF, and 1X
658 protease inhibitor cocktail (PIC - 0.174 mg/mL PMSF, 312 µg/mL benzamidine, 5 µg/mL
659 chymostatin, 5 µg/mL leupeptin, 1 µg/mL pepstatin A, 10 µg/mL aprotinin dissolved in
660 ethanol). After French Press (Avestin) lysis at 4 °C, the lysate was centrifuged twice for 30
661 min each. Polyethyleneimine (PEI, 10% (w/v) pH 8.0, Acros Organics – ThermoFisher
662 Scientific) was slowly added to the supernatant to a final concentration of ~0.6 % PEI with
663 continuous stirring. The mixture was stirred at 4 °C for an additional 25 min, then centrifuged
664 for 1.5h at 4 °C. The pellets were washed three times with 50 mM Tris-HCl pH 8.0, 500 mM
665 NaCl, 10 mM DTT, 5 % w/v glycerol, 1 mM PMSF, 1x PIC. For each wash, the pellets were
666 homogenized, then centrifuged again. RNA polymerase was eluted by washing the pellets
667 three times with 50 mM Tris-HCl pH 8.0, 1 M NaCl, 10 mM DTT, 5% w/v glycerol, 1x PIC,
668 1mM PMSF. The PEI elutions were combined and precipitated with ammonium sulfate, at a
669 final [$(NH_4)_2SO_4$] of 35% w/v, overnight. The mixture was centrifuged, and the pellets were
670 resuspended in 20 mM Tris-HCl pH 8.0, 1 M NaCl, 5% w/v glycerol, 1 mM 2-
671 mercaptoethanol (BME). The mixture was loaded onto two 5 mL HiTrap IMAC HP columns
672 (Cytiva) for a total column volume of 10 mL. RNA polymerase (β'-PPX-His_{10}) was eluted at
673 250 mM imidazole in column buffer (20 mM Tris-HCl pH 8.0, 1 M NaCl, 5% w/v glycerol, 1
674 mM BME). The eluted RNA polymerase fractions were combined and dialyzed to a final 10
675 mM Tris-HCl pH 8.0, 0.1 mM EDTA pH 8.0, 100 mM NaCl, 5% w/v glycerol, 5 mM DTT.
676 The sample was then loaded onto a 40 mL Bio-Rex-70 column (Bio-Rad), washed with 10
677 mM Tris-HCl pH 8.0, 0.1 mM EDTA, 5% w/v glycerol, 5 mM DTT in isocratic steps of
678 increasing NaCl concentration (elutes at 0.5M NaCl). The eluted fractions were combined,
679 concentrated by centrifugal filtration, then loaded onto a 320 mL HiLoad 26/600 Superdex
680 200 column (Cytiva) equilibrated in gel filtration buffer (10 mM Tris-HCl pH 8.0, 0.1 mM

681 EDTA pH 8.0, 0.5 M NaCl, 5 % w/v glycerol, 5 mM DTT). The eluted RNA polymerase was
682 concentrated to 8-10m g/mL by centrifugal concentration and supplemented with glycerol to
683 20% w/v, flash frozen in liquid N_2, and stored at −80°C.

684

685 **Expression and purification of *E. coli* σ^{70}**

686 Plasmid pSAD1403 was transformed into *E. coli* BL21(DE3). The cells were grown in the
687 presence of 50 µg/mL kanamycin to an OD_{600} of 0.6 at 37°C. Protein expression was induced
688 with 1 mM IPTG for 1-1.5h at 30 °C. Cells were harvested by centrifugation and resuspended
689 in 20 mM Tris-HCl pH 8.0, 500 mM NaCl, 0.1 mM EDTA pH 8.0, 5 mM imidazole, 5% w/v
690 glycerol, 0.5m M BME, 1 mM PMSF, 1x PIC (the same as used for the *E. coli* RNA
691 polymerase). After French Press, lysis at 4 °C, cell debris was removed by centrifugation twice.
692 The lysate was loaded onto two 5 mL HiTrap IMAC HP columns for a total column volume of
693 10mL. His_{10}-SUMO-σ^{70} was eluted at 250 mM imidazole in 20 mM Tris-HCl pH 8.0, 500 mM
694 NaCl, 0.1 mM EDTA pH 8.0, 5% w/v glycerol, 0.5 mM BME. Peak fractions were combined,
695 cleaved with Ulp1, and dialyzed against 20 mM Tris-HCl pH 8.0, 500 mM NaCl, 0.1 mM
696 EDTA pH 8.0, 5% w/v glycerol, 0.5 mM BME, resulting in a final imidazole concentration of
697 25 mM. The cleaved sample was loaded onto one 5 mL HiTrap IMAC HP to remove His_{10}-
698 SUMO-tag along with any remaining uncleaved σ^{70}. Untagged σ^{70} fractions were pooled and
699 diluted with 10mM Tris-HCl pH 8.0, 0.1 mM EDTA pH 8.0, 5% w/v glycerol, 1 mM DTT until
700 the conductivity corresponds to a NaCl concentration slightly below 200mM. The diluted
701 sample was injected on to three 5mL HiTrap Heparin HP columns (total column volume of 15
702 mL; Cytiva) equilibrated at the same diluent buffer but with 200 mM NaCl, and run a gradient
703 to 1 M NaCl, with the first major peak as the target peak. The target peak sample was pooled
704 and concentrated by centrifugal filtration before being loaded onto a HiLoad 16/60 Superdex
705 200 (Cytiva) in 20 mM Tris-HCl pH 8.0, 500 mM NaCl, 5% w/v glycerol, 1 mM DTT. Peak
706 fractions of σ^{70} were pooled, supplemented with glycerol to a final concentration of 20% w/v,
707 flash-frozen in liquid N_2, and stored at -80°C.

708

709 **Expression and purification of MtvS**

710 MtvS (FTN_1238) was cloned into pET21 with a C-terminal His_6-tag separated by a glycine
711 linker. MtvS overexpression was performed in *E. coli* Rosetta 2 (DE3). 2 l of bacteria were
712 grown to OD_{600} of 0.7 at 37 °C before the temperature was shifted to 16 °C and MtvS
713 expression was induced with 500 µM isopropyl β-d-1-thiogalactopyranoside (IPTG, GoldBio)
714 over night. Cells were harvested in 50 ml lysis buffer (50 mM HEPES pH 7.5, 250 mM NaCl,
715 10 % glycerol, 0.5 mg/ml lysozyme, 10 mM imidazole (Sigma-Aldrich), 1 mM TCEP-HCl,
716 mini cOmplete EDTA-free protease inhibitor cocktail) and lysed for 1 h at 4 °C shaking
717 before 15 rounds of sonication on ice (70 % amplitude, 10 s pulses, 30 s breaks). Cell lysate
718 was centrifuged at 18000 g, 4 °C for 1 h and the supernatant was filtrated with 0.45 µm filters
719 to remove remaining cell debris. After loading the cell lysate on a Nickel resin (HisPur Ni-
720 NTA, Thermo Fisher Scientific), column equilibrated with lysis buffer, two washes with 50
721 ml wash buffer (50 mM HEPES pH 7.5, 1 M NaCl, 10 % glycerol, 10 mM imidazole, 1 mM
722 TCEP-HCl) were carried out. Then MtvS-His_6 was eluted with 30 ml elution buffer (50 mM
723 HEPES pH 7.5, 250 mM NaCl, 10 % glycerol, 300 mM imidazole, 1 mM TCEP-HCl).
724 Elution was concentrated with 10 kDA cut-off filter (Amicon) and loaded on a Superdex 200
725 10/300-increase column (Cytiva) pre-equilibrated in size-exclusion buffer (50 mM HEPES

726 pH 7.5, 150 mM NaCl, 10 % glycerol, 1 mM TCEP-HCl) for further purification by size-
727 exclusion chromatography. Purified MtvS-His_6 was stored at -80 °C.

728

729 **Pull-down of *E. coli* RNA polymerase**

730 Interaction of MtvS-His_6 or FTN_1235-His_6 with *E. coli* RNA polymerase was probed as
731 described previously[89]. In short, purified MtvS-His_6 or FTN_1235-His_6 (20 µM) was
732 incubated with *E. coli* RNA polymerase core enzyme or holoenzyme (400 units/ml, NEB) in
733 40 µl reaction buffer (10 mM Tris-HCl pH 7.5, 50 mM KCl, 1 mM Dithiothreitol (GoldBio))
734 at 37 °C for 40 minutes. Afterwards, 260 µl of reaction buffer H (20 mM HEPES pH 7.5, 50
735 mM KCl, 10 mM imidazole, 0.001 % Triton-X (Sigma-Aldrich)) supplemented with 0.1
736 mg/ml bovum serum albumin (BSA, Sigma-Aldrich) was added to the reactions. 50 µl of
737 Dynabeads His-Tag Isolation and Pulldown beads per sample were washed twice with 300 µl
738 of reaction buffer H supplemented with BSA before the samples were transferred to the
739 prewashed beads and incubated on a roller at room temperature for 5 minutes. The beads were
740 washed once with 300 µl reaction buffer H supplemented with BSA and subsequently washed
741 three times with reaction buffer H. Afterwards, the proteins were eluted from the beads in 30
742 µl reaction buffer H containing 300 mM imidazole by incubating on a roller at room
743 temperature for 5 minutes. 15 µl of eluted samples and individual controls (MtvS-His_6 or
744 FTN_1235-His_6: 20 µg, *E. coli* RNA polymerase core enzyme and holoenzyme: 400 units/ml)
745 were analyzed on a SDS-PAGE gel and subsequent Coomassie staining.

746

747 ***In vitro* transcription assays**

748 *In vitro* transcription assays were based on a protocol reported previously[90]. Aptamer
749 sequences and primers are listed in table 8.

750 The spinach aptamer sequence flanked by first 32 base pairs of *cas12* and 32 base pairs of the
751 middle of *cas12* was ordered as gblock (Azenta). The gblock was cloned into an expression
752 vector flanked upstream by the amplified promoter sequence (400 bp upstream of gene of
753 interest) and the *E. coli rrnnB T1* terminator. Linearized aptamers were amplified from
754 plasmid, cleaned up (Qiagen) and eluted in H_2O.

755 The storage buffer of recombinant *E. coli* RNA polymerase and σ^{70} as well as *F. novicida*
756 MtvS was exchanged to transcription buffer (50 mM Tris-HCl pH8, 150 mM KCl, 10 mM
757 $MgCl_2$, 1 mM Dithiothreitol, 0.1 mg/ml BSA) with desalting columns (Zeba, 7K MWCO, 0.5
758 ml). In short, the columns were centrifuged at 1500 g for 1 minute at 4 °C to expel the storage
759 buffer. Then the columns were washed two times with 300 µl transcription buffer
760 supplemented with 0.01 % Tween-20 (Millipore). The last wash was performed with 300 µl
761 transcription buffer only. The proteins resuspended in 50-100 µl transcription buffer were
762 added to the columns and recovered in fresh tubes.

763 Complexes of *E. coli* RNA polymerase (500 nM) with *E. coli* σ^{70} (2500 nM) or MtvS (2500
764 nM) were reconstituted by mixing them in a 1:5:5 ratio in transcription buffer followed by an
765 incubation at 37 °C for 40 minutes.

766 The *in vitro* transcription assays were carried out in black 384-well plates (Corning, low
767 volume black round bottom polystyrene NBS) in technical triplicates and "no NTP" controls.
768 First, 10 nM aptamer DNA, 0.4 U/µl RiboLock RNAse inhibitor (Thermo Fisher Scientific),
769 0.5 mM NTPs (Thermo Fisher Scientific) and 20 µM 3,5-difluoro-4-hydroxybenzylidene
770 imidazolinone (DFHBI, Lucerna) in 15 µl transcription buffer was added to each wells. Then
771 the plate was incubated at 37 °C in the dark for 10 minutes before 50 nM RNA polymerase

complexes (5 µl of the reconstituted complexes) were added. The "no NTP" controls contained everything except for the NTPs. Measurement of fluorescence (excitation: 470 nm, emission: 528 nm) in a plate reader started immediately after adding the RNA polymerase complexes. Measurements were taken every 30 seconds for 1 h.

Homology prediction with Foldseek

Foldseek was used to find structural homologs for the predicted structure of MtvS (FTN_1238, Uniprot ID: A0A6I4RTR9)[91]. PyMol (v 2.5.7) was used to generate figures[92].

Heatmaps

The normalized counts and normalized log2 iBAQ values were used to create heatmaps for genes and proteins which were deemed significant (adj*p*-value < 0.05) with heatmap2 on usegalaxy.org[93,94]. Z-scores were computed on rows before clustering.

Gene set enrichment analysis (GSEA)

Gense set enrichment analysis was carried out with the FUNAGE-Pro[95] (v2) online tool using the genbank file ASM1464v1. Only genes with an adj*p* value ≤ 0.05 were considered and upregulated and downregulated genes were analyzed separately. For RNA-seq data sets, ribosomal RNAs were excluded. For comparison of RNA levels between the two growth conditions for the parental strain, the threshold values were set to -1.5 > log2FC > 1.5. For comparison of RNA levels between the parental strain and the *mtvS ns* mutant, the threshold values were set to -1 > log2FC > 1. Enriched pathways for each strain and condition are listed in table 15. For comparison of protein levels between the two growth phases for the parental strain, the threshold values were set to -1> log2FC > 1. For comparison of protein levels between parental strain and *mtvS ns* mutant, the threshold values were set to -0.5 > log2FC > 0.5. Enriched pathways for each strain and condition are listed in table 11.

Sequence alignments

Promoter sequences of operons significantly down regulated according to FUNAGE-Pro were aligned with MEGA12 using the ClustalW algorithm[96]. The sequence logo plot of the putative -35 consensus sequence was created using WebLogo[97].

Protein sequences of MtvS (A0A6I4RTR9) and *E. coli* YgfB (P0A8C4) were aligned with MEGA12 using the ClustalW alogrithm.

Structural predictions with AlphaFold 3

Interactions between MtvS (AlphaFold ID: A0A6I4RTR9) and *F. novicida* U112 RNA polymerase (AlphaFold IDs: RpoA1 - A0Q4K8, RpoA2 - A0Q7R6, RpoB - A0Q867, RpoC - A0Q866, RpoZ - A0Q5J3) were predicted with the AlphaFold 3 web server (https://alphafoldserver.com)[50].

Interactions between the coiled-coil domain of β' subunit (RpoC) and σ^{70} or MtvS were compared using AlphaFold 3 predictions of *E. coli* RNA polymerase (AlphaFold ID: RpoA - P0A7Z4, RpoB - P0A8V2, RpoC - P0A8T7, RpoZ - P0A800) with *E. coli* σ^{70} (AlphaFold ID: RpoD - P00579) or MtvS (AlphaFold ID: A0A6I4RTR9. The magnesium ion was superimposed from the solved *E. coli* RNA polymerase structure (6omf)[98].

816 For assessment of prediction accuracy, the PAE values and and ipTM and pTM scores were
817 taken into account according to the guidelines.

818 PyMol (v 2.5.7)[92] was used to generate figures and determine interactions under 3 Å between
819 MtvS and RpoC.

820 **Data availability**

821 Source data are provided in this paper.

822 **References**

823 1. Marraffini, L.A., and Sontheimer, E.J. (2008). CRISPR interference limits horizontal
824 gene transfer in staphylococci by targeting DNA. Science *322*, 1843–1845.
825 https://doi.org/10.1126/science.1165771.

826 2. Barrangou, R., Fremaux, C., Deveau, H., Richards, M., Boyaval, P., Moineau, S.,
827 Romero, D.A., and Horvath, P. (2007). CRISPR provides acquired resistance against viruses
828 in prokaryotes. Science *315*, 1709–1712. https://doi.org/10.1126/science.1138140.

829 3. Bolotin, A., Quinquis, B., Sorokin, A., and Ehrlich, S.D. 2005 Clustered regularly
830 interspaced short palindrome repeats (CRISPRs) have spacers of extrachromosomal origin.
831 Microbiology *151*, 2551–2561. https://doi.org/10.1099/mic.0.28048-0.

832 4. Mojica, F.J.M., Díez-Villaseñor, C., García-Martínez, J., and Soria, E. (2005).
833 Intervening Sequences of Regularly Spaced Prokaryotic Repeats Derive from Foreign Genetic
834 Elements. J. Mol. Evol. *60*, 174–182. https://doi.org/10.1007/s00239-004-0046-3.

835 5. Pourcel, C., Salvignol, G., and Vergnaud, G.Y. 2005 CRISPR elements in Yersinia
836 pestis acquire new repeats by preferential uptake of bacteriophage DNA, and provide
837 additional tools for evolutionary studies. Microbiology *151*, 653–663.
838 https://doi.org/10.1099/mic.0.27437-0.

839 6. Brouns, S.J.J., Jore, M.M., Lundgren, M., Westra, E.R., Slijkhuis, R.J.H., Snijders,
840 A.P.L., Dickman, M.J., Makarova, K.S., Koonin, E.V., and Oost, J. van der (2008). Small
841 CRISPR RNAs Guide Antiviral Defense in Prokaryotes. Science.
842 https://doi.org/10.1126/science.1159689.

843 7. Hale, C., Kleppe, K., Terns, R.M., and Terns, M.P. (2008). Prokaryotic silencing
844 (psi)RNAs in Pyrococcus furiosus. RNA N. Y. N *14*, 2572–2579.
845 https://doi.org/10.1261/rna.1246808.

846 8. Abudayyeh, O.O., Gootenberg, J.S., Konermann, S., Joung, J., Slaymaker, I.M., Cox,
847 D.B.T., Shmakov, S., Makarova, K.S., Semenova, E., Minakhin, L., et al. (2016). C2c2 is a
848 single-component programmable RNA-guided RNA-targeting CRISPR effector. Science *353*,
849 aaf5573. https://doi.org/10.1126/science.aaf5573.

850 9. Gasiunas, G., Barrangou, R., Horvath, P., and Siksnys, V. (2012). Cas9-crRNA
851 ribonucleoprotein complex mediates specific DNA cleavage for adaptive immunity in
852 bacteria. Proc. Natl. Acad. Sci. U. S. A. *109*, E2579-2586.
853 https://doi.org/10.1073/pnas.1208507109.

854 10. Hale, C.R., Zhao, P., Olson, S., Duff, M.O., Graveley, B.R., Wells, L., Terns, R.M.,
855 and Terns, M.P. (2009). RNA-Guided RNA Cleavage by a CRISPR RNA-Cas Protein
856 Complex. Cell *139*, 945–956. https://doi.org/10.1016/j.cell.2009.07.040.

857 11. Jinek, M., Chylinski, K., Fonfara, I., Hauer, M., Doudna, J.A., and Charpentier, E.
858 (2012). A programmable dual-RNA-guided DNA endonuclease in adaptive bacterial
859 immunity. Science *337*, 816–821. https://doi.org/10.1126/science.1225829.

860 12. Westra, E.R., van Erp, P.B.G., Künne, T., Wong, S.P., Staals, R.H.J., Seegers, C.L.C.,
861 Bollen, S., Jore, M.M., Semenova, E., Severinov, K., et al. (2012). CRISPR immunity relies

862 on the consecutive binding and degradation of negatively supercoiled invader DNA by
863 Cascade and Cas3. Mol. Cell *46*, 595–605. https://doi.org/10.1016/j.molcel.2012.03.018.

864 13. Zetsche, B., Gootenberg, J.S., Abudayyeh, O.O., Slaymaker, I.M., Makarova, K.S.,
865 Essletzbichler, P., Volz, S.E., Joung, J., van der Oost, J., Regev, A., et al. (2015). Cpf1 is a
866 single RNA-guided endonuclease of a class 2 CRISPR-Cas system. Cell *163*, 759–771.
867 https://doi.org/10.1016/j.cell.2015.09.038.

868 14. Makarova, K.S., Wolf, Y.I., Iranzo, J., Shmakov, S.A., Alkhnbashi, O.S., Brouns,
869 S.J.J., Charpentier, E., Cheng, D., Haft, D.H., Horvath, P., et al. (2020). Evolutionary
870 classification of CRISPR-Cas systems: a burst of class 2 and derived variants. Nat. Rev.
871 Microbiol. *18*, 67–83. https://doi.org/10.1038/s41579-019-0299-x.

872 15. Patterson, A.G., Jackson, S.A., Taylor, C., Evans, G.B., Salmond, G.P.C., Przybilski,
873 R., Staals, R.H.J., and Fineran, P.C. (2016). Quorum Sensing Controls Adaptive Immunity
874 through the Regulation of Multiple CRISPR-Cas Systems. Mol. Cell *64*, 1102–1108.
875 https://doi.org/10.1016/j.molcel.2016.11.012.

876 16. Høyland-Kroghsbo, N.M., Paczkowski, J., Mukherjee, S., Broniewski, J., Westra, E.,
877 Bondy-Denomy, J., and Bassler, B.L. (2017). Quorum sensing controls the Pseudomonas
878 aeruginosa CRISPR-Cas adaptive immune system. Proc. Natl. Acad. Sci. U. S. A. *114*, 131–
879 135. https://doi.org/10.1073/pnas.1617415113.

880 17. Lucas-Elío, P., Molina-Quintero, L.R., Xu, H., and Sánchez-Amat, A. (2021). A
881 histidine kinase and a response regulator provide phage resistance to Marinomonas
882 mediterranea via CRISPR-Cas regulation. Sci. Rep. *11*, 20564.
883 https://doi.org/10.1038/s41598-021-99740-9.

884 18. Borges, A.L., Castro, B., Govindarajan, S., Solvik, T., Escalante, V., and Bondy-
885 Denomy, J. (2020). Bacterial alginate regulators and phage homologs repress CRISPR-Cas
886 immunity. Nat. Microbiol. *5*, 679–687. https://doi.org/10.1038/s41564-020-0691-3.

887 19. Perez-Rodriguez, R., Haitjema, C., Huang, Q., Nam, K.H., Bernardis, S., Ke, A., and
888 DeLisa, M.P. (2011). Envelope stress is a trigger of CRISPR RNA-mediated DNA silencing
889 in Escherichia coli. Mol. Microbiol. *79*, 584–599. https://doi.org/10.1111/j.1365-
890 2958.2010.07482.x.

891 20. Pul, U., Wurm, R., Arslan, Z., Geissen, R., Hofmann, N., and Wagner, R. (2010).
892 Identification and characterization of E. coli CRISPR-cas promoters and their silencing by H-
893 NS. Mol. Microbiol. *75*, 1495–1512. https://doi.org/10.1111/j.1365-2958.2010.07073.x.

894 21. Westra, E.R., Pul, U., Heidrich, N., Jore, M.M., Lundgren, M., Stratmann, T., Wurm,
895 R., Raine, A., Mescher, M., Van Heereveld, L., et al. (2010). H-NS-mediated repression of
896 CRISPR-based immunity in Escherichia coli K12 can be relieved by the transcription
897 activator LeuO. Mol. Microbiol. *77*, 1380–1393. https://doi.org/10.1111/j.1365-
898 2958.2010.07315.x.

899 22. Kang, D.-Y., Kim, A., and Kim, J.N. (2023). CcpA and CodY Regulate CRISPR-Cas
900 System of Streptococcus mutans. Microbiol. Spectr., e0182623.
901 https://doi.org/10.1128/spectrum.01826-23.

902 23. Smith, L.M., Hampton, H.G., Yevstigneyeva, M.S., Mahler, M., Paquet, Z.S.M., and
903 Fineran, P.C. (2023). CRISPR-Cas immunity is repressed by the LysR-type transcriptional
904 regulator PigU. Nucleic Acids Res., gkad1165. https://doi.org/10.1093/nar/gkad1165.

905 24. Zhang, Y., Yang, J., and Bai, G. (2018). Regulation of the CRISPR-Associated Genes
906 by Rv2837c (CnpB) via an Orn-Like Activity in Tuberculosis Complex Mycobacteria. J.
907 Bacteriol. *200*, e00743-17. https://doi.org/10.1128/JB.00743-17.

908 25. Patterson, A.G., Chang, J.T., Taylor, C., and Fineran, P.C. (2015). Regulation of the
909 Type I-F CRISPR-Cas system by CRP-cAMP and GalM controls spacer acquisition and
910 interference. Nucleic Acids Res. *43*, 6038–6048. https://doi.org/10.1093/nar/gkv517.

911 26. Smith, L.M., Jackson, S.A., Malone, L.M., Ussher, J.E., Gardner, P.P., and Fineran,
912 P.C. (2021). The Rcs stress response inversely controls surface and CRISPR-Cas adaptive
913 immunity to discriminate plasmids and phages. Nat. Microbiol. *6*, 162–172.
914 https://doi.org/10.1038/s41564-020-00822-7.

915 27. Medina-Aparicio, L., Rebollar-Flores, J.E., Gallego-Hernández, A.L., Vázquez, A.,
916 Olvera, L., Gutiérrez-Ríos, R.M., Calva, E., and Hernández-Lucas, I. (2011). The
917 CRISPR/Cas immune system is an operon regulated by LeuO, H-NS, and leucine-responsive
918 regulatory protein in Salmonella enterica serovar Typhi. J. Bacteriol. *193*, 2396–2407.
919 https://doi.org/10.1128/JB.01480-10.

920 28. He, F., Vestergaard, G., Peng, W., She, Q., and Peng, X. (2017). CRISPR-Cas type I-
921 A Cascade complex couples viral infection surveillance to host transcriptional regulation in
922 the dependence of Csa3b. Nucleic Acids Res. *45*, 1902–1913.
923 https://doi.org/10.1093/nar/gkw1265.

924 29. Shmakov, S.A., Barth, Z.K., Makarova, K.S., Wolf, Y.I., Brover, V., Peters, J.E., and
925 Koonin, E.V. (2023). Widespread CRISPR repeat-like RNA regulatory elements in CRISPR-
926 Cas systems. Preprint at bioRxiv, https://doi.org/10.1101/2023.03.03.530964
927 https://doi.org/10.1101/2023.03.03.530964.

928 30. Liu, C., Wang, R., Li, J., Cheng, F., Shu, X., Zhao, H., Xue, Q., Yu, H., Wu, A.,
929 Wang, L., et al. (2023). Widespread RNA-based cas regulation monitors crRNA abundance
930 and anti-CRISPR proteins. Cell Host Microbe *31*, 1481-1493.e6.
931 https://doi.org/10.1016/j.chom.2023.08.005.

932 31. Workman, R.E., Pammi, T., Nguyen, B.T.K., Graeff, L.W., Smith, E., Sebald, S.M.,
933 Stoltzfus, M.J., Euler, C.W., and Modell, J.W. (2021). A natural single-guide RNA
934 repurposes Cas9 to autoregulate CRISPR-Cas expression. Cell *184*, 675-688.e19.
935 https://doi.org/10.1016/j.cell.2020.12.017.

936 32. Liu, T., Li, Y., Wang, X., Ye, Q., Li, H., Liang, Y., She, Q., and Peng, N. (2015).
937 Transcriptional regulator-mediated activation of adaptation genes triggers CRISPR de novo
938 spacer acquisition. Nucleic Acids Res. *43*, 1044–1055. https://doi.org/10.1093/nar/gku1383.

939 33. Maharajan, A.D., Hjerde, E., Hansen, H., and Willassen, N.P. (2022). Quorum
940 Sensing Controls the CRISPR and Type VI Secretion Systems in Aliivibrio wodanis
941 06/09/139. Front. Vet. Sci. *9*, 799414. https://doi.org/10.3389/fvets.2022.799414.

942 34. Bilger, R., Migur, A., Wulf, A., Steglich, C., Urlaub, H., and Hess, W.R. (2024). A
943 type III-Dv CRISPR-Cas system is controlled by the transcription factor RpaB and interacts

944 with the DEAD-box RNA helicase CrhR. Cell Rep. *43*, 114485.
945 https://doi.org/10.1016/j.celrep.2024.114485.

946 35. Kim, H., and Marraffini, L.A. (2024). Cas9 interaction with the tracrRNA nexus
947 modulates the repression of type II-A CRISPR-cas genes. Nucleic Acids Res., gkae597.
948 https://doi.org/10.1093/nar/gkae597.

949 36. Schunder, E., Rydzewski, K., Grunow, R., and Heuner, K. (2013). First indication for
950 a functional CRISPR/Cas system in Francisella tularensis. Int. J. Med. Microbiol. IJMM *303*,
951 51–60. https://doi.org/10.1016/j.ijmm.2012.11.004.

952 37. Fonfara, I., Richter, H., Bratovič, M., Le Rhun, A., and Charpentier, E. (2016). The
953 CRISPR-associated DNA-cleaving enzyme Cpf1 also processes precursor CRISPR RNA.
954 Nature *532*, 517–521. https://doi.org/10.1038/nature17945.

955 38. Ratner, H.K., and Weiss, D.S. (2020). F. novicida CRISPR-Cas systems can
956 functionally complement each other in DNA defense while providing target flexibility. J.
957 Bacteriol. https://doi.org/10.1128/JB.00670-19.

958 39. Ratner, H.K., and Weiss, D.S. (2021). crRNA complementarity shifts endogenous
959 CRISPR-Cas systems between transcriptional repression and DNA defense. RNA Biol., 1–14.
960 https://doi.org/10.1080/15476286.2021.1878335.

961 40. Sampson, T.R., Saroj, S.D., Llewellyn, A.C., Tzeng, Y.-L., and Weiss, D.S. (2013). A
962 CRISPR/Cas system mediates bacterial innate immune evasion and virulence. Nature *497*,
963 254–257. https://doi.org/10.1038/nature12048.

964 41. Sampson, T.R., Saroj, S.D., Llewellyn, A.C., Tzeng, Y.-L., and Weiss, D.S. (2019).
965 Author Correction: A CRISPR/Cas system mediates bacterial innate immune evasion and
966 virulence. Nature *570*, E30–E31. https://doi.org/10.1038/s41586-019-1253-9.

967 42. Sampson, T.R., Napier, B.A., Schroeder, M.R., Louwen, R., Zhao, J., Chin, C.-Y.,
968 Ratner, H.K., Llewellyn, A.C., Jones, C.L., Laroui, H., et al. (2014). A CRISPR-Cas system
969 enhances envelope integrity mediating antibiotic resistance and inflammasome evasion. Proc.
970 Natl. Acad. Sci. U. S. A. *111*, 11163–11168. https://doi.org/10.1073/pnas.1323025111.

971 43. Ratner, H.K., Escalera-Maurer, A., Le Rhun, A., Jaggavarapu, S., Wozniak, J.E.,
972 Crispell, E.K., Charpentier, E., and Weiss, D.S. (2019). Catalytically Active Cas9 Mediates
973 Transcriptional Interference to Facilitate Bacterial Virulence. Mol. Cell *75*, 498-510.e5.
974 https://doi.org/10.1016/j.molcel.2019.05.029.

975 44. Dai, S., Mohapatra, N.P., Schlesinger, L.S., and Gunn, J.S. (2010). Regulation of
976 francisella tularensis virulence. Front. Microbiol. *1*, 144.
977 https://doi.org/10.3389/fmicb.2010.00144.

978 45. Feklístov, A., Sharon, B.D., Darst, S.A., and Gross, C.A. (2014). Bacterial sigma
979 factors: a historical, structural, and genomic perspective. Annu. Rev. Microbiol. *68*, 357–376.
980 https://doi.org/10.1146/annurev-micro-092412-155737.

981 46. Charity, J.C., Costante-Hamm, M.M., Balon, E.L., Boyd, D.H., Rubin, E.J., and Dove,
982 S.L. (2007). Twin RNA polymerase-associated proteins control virulence gene expression in
983 Francisella tularensis. PLoS Pathog. *3*, e84. https://doi.org/10.1371/journal.ppat.0030084.

984 47. Mukhamedyarov, D., Makarova, K.S., Severinov, K., and Kuznedelov, K. (2011).
985 Francisella RNA polymerase contains a heterodimer of non-identical α subunits. BMC Mol.
986 Biol. *12*, 50. https://doi.org/10.1186/1471-2199-12-50.

987 48. Travis, B.A., Ramsey, K.M., Prezioso, S.M., Tallo, T., Wandzilak, J.M., Hsu, A.,
988 Borgnia, M., Bartesaghi, A., Dove, S.L., Brennan, R.G., et al. (2021). Structural Basis for
989 Virulence Activation of Francisella tularensis. Mol. Cell *81*, 139-152.e10.
990 https://doi.org/10.1016/j.molcel.2020.10.035.

991 49. Bell, R.T., Wolf, Y.I., and Koonin, E.V. (2020). Modified base-binding EVE and
992 DCD domains: striking diversity of genomic contexts in prokaryotes and predicted
993 involvement in a variety of cellular processes. BMC Biol. *18*, 159.
994 https://doi.org/10.1186/s12915-020-00885-2.

995 50. Abramson, J., Adler, J., Dunger, J., Evans, R., Green, T., Pritzel, A., Ronneberger, O.,
996 Willmore, L., Ballard, A.J., Bambrick, J., et al. (2024). Accurate structure prediction of
997 biomolecular interactions with AlphaFold 3. Nature *630*, 493–500.
998 https://doi.org/10.1038/s41586-024-07487-w.

999 51. Campbell, E.A., Muzzin, O., Chlenov, M., Sun, J.L., Olson, C.A., Weinman, O.,
1000 Trester-Zedlitz, M.L., and Darst, S.A. (2002). Structure of the bacterial RNA polymerase
1001 promoter specificity sigma subunit. Mol. Cell *9*, 527–539. https://doi.org/10.1016/s1097-
1002 2765(02)00470-7.

1003 52. Feklistov, A., and Darst, S.A. (2011). Structural basis for promoter-10 element
1004 recognition by the bacterial RNA polymerase σ subunit. Cell *147*, 1257–1269.
1005 https://doi.org/10.1016/j.cell.2011.10.041.

1006 53. Malhotra, A., Severinova, E., and Darst, S.A. (1996). Crystal structure of a sigma 70
1007 subunit fragment from E. coli RNA polymerase. Cell *87*, 127–136.
1008 https://doi.org/10.1016/s0092-8674(00)81329-x.

1009 54. Lonetto, M.A., Brown, K.L., Rudd, K.E., and Buttner, M.J. (1994). Analysis of the
1010 Streptomyces coelicolor sigE gene reveals the existence of a subfamily of eubacterial RNA
1011 polymerase sigma factors involved in the regulation of extracytoplasmic functions. Proc. Natl.
1012 Acad. Sci. U. S. A. *91*, 7573–7577. https://doi.org/10.1073/pnas.91.16.7573.

1013 55. Léonetti, J.P., Wong, K., and Geiduschek, E.P. (1998). Core-sigma interaction:
1014 probing the interaction of the bacteriophage T4 gene 55 promoter recognition protein with
1015 E.coli RNA polymerase core. EMBO J. *17*, 1467–1475.
1016 https://doi.org/10.1093/emboj/17.5.1467.

1017 56. Helmann, J.D. (2016). *Bacillus subtilis* extracytoplasmic function (ECF) sigma factors
1018 and defense of the cell envelope. Curr. Opin. Microbiol. *30*, 122–132.
1019 https://doi.org/10.1016/j.mib.2016.02.002.

1020 57. Lonetto, M., Gribskov, M., and Gross, C.A. (1992). The sigma 70 family: sequence
1021 conservation and evolutionary relationships. J. Bacteriol. *174*, 3843–3849.
1022 https://doi.org/10.1128/jb.174.12.3843-3849.1992.

1023 58. Tan, D., Svenningsen, S.L., and Middelboe, M. (2015). Quorum Sensing Determines
1024 the Choice of Antiphage Defense Strategy in Vibrio anguillarum. mBio *6*, e00627.
1025 https://doi.org/10.1128/mBio.00627-15.

1026 59. Gao, R., Krysciak, D., Petersen, K., Utpatel, C., Knapp, A., Schmeisser, C., Daniel, R.,
1027 Voget, S., Jaeger, K.-E., and Streit, W.R. (2015). Genome-wide RNA sequencing analysis of
1028 quorum sensing-controlled regulons in the plant-associated Burkholderia glumae PG1 strain.
1029 Appl. Environ. Microbiol. *81*, 7993–8007. https://doi.org/10.1128/AEM.01043-15.

1030 60. Dela Ahator, S., Liu, Y., Wang, J., and Zhang, L.-H. (2022). The virulence factor
1031 regulator and quorum sensing regulate the type I-F CRISPR-Cas mediated horizontal gene
1032 transfer in Pseudomonas aeruginosa. Front. Microbiol. *13*, 987656.
1033 https://doi.org/10.3389/fmicb.2022.987656.

1034 61. Nuñez, J.K., Bai, L., Harrington, L.B., Hinder, T.L., and Doudna, J.A. (2016).
1035 CRISPR Immunological Memory Requires a Host Factor for Specificity. Mol. Cell *62*, 824–
1036 833. https://doi.org/10.1016/j.molcel.2016.04.027.

1037 62. Ali Azam, T., Iwata, A., Nishimura, A., Ueda, S., and Ishihama, A. (1999). Growth
1038 phase-dependent variation in protein composition of the Escherichia coli nucleoid. J.
1039 Bacteriol. *181*, 6361–6370. https://doi.org/10.1128/JB.181.20.6361-6370.1999.

1040 63. Kretz, J., Börner, J., Friedrich, T., McIntosh, M., Procida-Kowalski, T., Gerken, F.,
1041 Wilhelm, J., and Klug, G. (2024). Function of the RNA-targeting class 2 type VI CRISPR Cas
1042 system of Rhodobacter capsulatus. Front. Microbiol. *15*, 1384543.
1043 https://doi.org/10.3389/fmicb.2024.1384543.

1044 64. Høyland-Kroghsbo, N.M., Maerkedahl, R.B., and Svenningsen, S.L. (2013). A
1045 quorum-sensing-induced bacteriophage defense mechanism. mBio *4*, e00362-00312.
1046 https://doi.org/10.1128/mBio.00362-12.

1047 65. Galkin, A., Sarikaya, E., Lehmann, C., Howard, A., and Herzberg, O. (2004). X-ray
1048 structure of HI0817 from Haemophilus influenzae: protein of unknown function with a novel
1049 fold. Proteins *57*, 874–877. https://doi.org/10.1002/prot.20260.

1050 66. Eggers, O., Renschler, F.A., Michalek, L.A., Wackler, N., Walter, E., Smollich, F.,
1051 Klein, K., Sonnabend, M.S., Egle, V., Angelov, A., et al. (2023). YgfB increases β-lactam
1052 resistance in Pseudomonas aeruginosa by counteracting AlpA-mediated ampDh3 expression.
1053 Commun. Biol. *6*, 254. https://doi.org/10.1038/s42003-023-04609-4.

1054 67. Sonnabend, M.S., Klein, K., Beier, S., Angelov, A., Kluj, R., Mayer, C., Groß, C.,
1055 Hofmeister, K., Beuttner, A., Willmann, M., et al. (2020). Identification of Drug Resistance
1056 Determinants in a Clinical Isolate of Pseudomonas aeruginosa by High-Density Transposon
1057 Mutagenesis. Antimicrob. Agents Chemother. *64*, e01771-19.
1058 https://doi.org/10.1128/AAC.01771-19.

1059 68. Arthur, T.M., Anthony, L.C., and Burgess, R.R. (2000). Mutational Analysis of β′260–
1060 309, a ς70 Binding Site Located on Escherichia coliCore RNA Polymerase *. J. Biol. Chem.
1061 *275*, 23113–23119. https://doi.org/10.1074/jbc.M002040200.

1062 69. Young, B.A., Anthony, L.C., Gruber, T.M., Arthur, T.M., Heyduk, E., Lu, C.Z.,
1063 Sharp, M.M., Heyduk, T., Burgess, R.R., and Gross, C.A. (2001). A coiled-coil from the
1064 RNA polymerase beta' subunit allosterically induces selective nontemplate strand binding by
1065 sigma(70). Cell *105*, 935–944. https://doi.org/10.1016/s0092-8674(01)00398-1.

1066 70. Murakami, K.S., Masuda, S., and Darst, S.A. (2002). Structural basis of transcription
1067 initiation: RNA polymerase holoenzyme at 4 A resolution. Science *296*, 1280–1284.
1068 https://doi.org/10.1126/science.1069594.

1069 71. Twist, K.-A.F., Campbell, E.A., Deighan, P., Nechaev, S., Jain, V., Geiduschek, E.P.,
1070 Hochschild, A., and Darst, S.A. (2011). Crystal structure of the bacteriophage T4 late-
1071 transcription coactivator gp33 with the β-subunit flap domain of Escherichia coli RNA
1072 polymerase. Proc. Natl. Acad. Sci. U. S. A. *108*, 19961–19966.
1073 https://doi.org/10.1073/pnas.1113328108.

1074 72. Nechaev, S., Kamali-Moghaddam, M., André, E., Léonetti, J.-P., and Geiduschek, E.P.
1075 (2004). The bacteriophage T4 late-transcription coactivator gp33 binds the flap domain of
1076 Escherichia coli RNA polymerase. Proc. Natl. Acad. Sci. U. S. A. *101*, 17365–17370.
1077 https://doi.org/10.1073/pnas.0408028101.

1078 73. Kassavetis, G.A., and Geiduschek, E.P. (1984). Defining a bacteriophage T4 late
1079 promoter: bacteriophage T4 gene 55 protein suffices for directing late promoter recognition.
1080 Proc. Natl. Acad. Sci. U. S. A. *81*, 5101–5105. https://doi.org/10.1073/pnas.81.16.5101.

1081 74. Grall, N., Livny, J., Waldor, M., Barel, M., Charbit, A., and Meibom, K.L. (2009).
1082 Pivotal role of the Francisella tularensis heat-shock sigma factor RpoH. Microbiol. Read.
1083 Engl. *155*, 2560–2572. https://doi.org/10.1099/mic.0.029058-0.

1084 75. Surette, M.G., and Bassler, B.L. (1998). Quorum sensing in Escherichia coli and
1085 Salmonella typhimurium. Proc. Natl. Acad. Sci. U. S. A. *95*, 7046–7050.
1086 https://doi.org/10.1073/pnas.95.12.7046.

1087 76. van Hoek, M.L., Hoang, K.V., and Gunn, J.S. (2019). Two-Component Systems in
1088 Francisella Species. Front. Cell. Infect. Microbiol. *9*, 198.
1089 https://doi.org/10.3389/fcimb.2019.00198.

1090 77. Lindgren, H., Shen, H., Zingmark, C., Golovliov, I., Conlan, W., and Sjöstedt, A.
1091 (2007). Resistance of Francisella tularensis strains against reactive nitrogen and oxygen
1092 species with special reference to the role of KatG. Infect. Immun. *75*, 1303–1309.
1093 https://doi.org/10.1128/IAI.01717-06.

1094 78. Brodmann, M., Dreier, R.F., Broz, P., and Basler, M. (2017). Francisella requires
1095 dynamic type VI secretion system and ClpB to deliver effectors for phagosomal escape. Nat.
1096 Commun. *8*, 15853. https://doi.org/10.1038/ncomms15853.

1097 79. Brodmann, M., Heilig, R., Broz, P., and Basler, M. (2018). Mobilizable Plasmids for
1098 Tunable Gene Expression in Francisella novicida. Front. Cell. Infect. Microbiol. *8*.
1099 https://doi.org/10.3389/fcimb.2018.00284.

1100 80. Harms, A., Segers, F.H.I.D., Quebatte, M., Mistl, C., Manfredi, P., Körner, J., Chomel,
1101 B.B., Kosoy, M., Maruyama, S., Engel, P., et al. (2017). Evolutionary Dynamics of
1102 Pathoadaptation Revealed by Three Independent Acquisitions of the VirB/D4 Type IV
1103 Secretion System in Bartonella. Genome Biol. Evol. *9*, 761–776.
1104 https://doi.org/10.1093/gbe/evx042.

1105 81. Schindelin, J., Arganda-Carreras, I., Frise, E., Kaynig, V., Longair, M., Pietzsch, T.,
1106 Preibisch, S., Rueden, C., Saalfeld, S., Schmid, B., et al. (2012). Fiji: an open-source platform
1107 for biological-image analysis. Nat. Methods *9*, 676–682. https://doi.org/10.1038/nmeth.2019.

1108 82. Aranda, P.S., LaJoie, D.M., and Jorcyk, C.L. (2012). Bleach gel: a simple agarose gel
1109 for analyzing RNA quality. Electrophoresis *33*, 366–369.
1110 https://doi.org/10.1002/elps.201100335.

1111 83. Rohmer, L., Fong, C., Abmayr, S., Wasnick, M., Larson Freeman, T.J., Radey, M.,
1112 Guina, T., Svensson, K., Hayden, H.S., Jacobs, M., et al. (2007). Comparison of Francisella
1113 tularensis genomes reveals evolutionary events associated with the emergence of human
1114 pathogenic strains. Genome Biol. *8*, R102. https://doi.org/10.1186/gb-2007-8-6-r102.

1115 84. Magoc, T., Wood, D., and Salzberg, S.L. (2013). EDGE-pro: Estimated Degree of
1116 Gene Expression in Prokaryotic Genomes. Evol. Bioinforma. Online *9*, 127–136.
1117 https://doi.org/10.4137/EBO.S11250.

1118 85. Love, M.I., Huber, W., and Anders, S. (2014). Moderated estimation of fold change
1119 and dispersion for RNA-seq data with DESeq2. Genome Biol. *15*, 550.
1120 https://doi.org/10.1186/s13059-014-0550-8.

1121 86. Llewellyn, A.C., Jones, C.L., Napier, B.A., Bina, J.E., and Weiss, D.S. (2011).
1122 Macrophage replication screen identifies a novel Francisella hydroperoxide resistance protein
1123 involved in virulence. PloS One *6*, e24201. https://doi.org/10.1371/journal.pone.0024201.

1124 87. Chaparian, R.R., and van Kessel, J.C. (2021). Promoter Pull-Down Assay: A
1125 Biochemical Screen for DNA-Binding Proteins. Methods Mol. Biol. Clifton NJ *2346*, 165–
1126 172. https://doi.org/10.1007/7651_2020_307.

1127 88. Jutras, B.L., Verma, A., and Stevenson, B. (2012). Identification of novel DNA-
1128 binding proteins using DNA-affinity chromatography/pull down. Curr. Protoc. Microbiol.
1129 *Chapter 1*, Unit1F.1. https://doi.org/10.1002/9780471729259.mc01f01s24.

1130 89. Smalakyte, D., Ruksenaite, A., Sasnauskas, G., Tamulaitiene, G., and Tamulaitis, G.
1131 (2024). Filament formation activates protease and ring nuclease activities of CRISPR Lon-
1132 SAVED. Mol. Cell *84*, 4239-4255.e8. https://doi.org/10.1016/j.molcel.2024.09.002.

1133 90. Jensen, D., Ruiz Manzano, A., Rector, M., Tomko, E.J., Record, M.T., and Galburt,
1134 E.A. (2023). High-throughput, fluorescent-aptamer-based measurements of steady-state
1135 transcription rates for the Mycobacterium tuberculosis RNA polymerase. Nucleic Acids Res.
1136 *51*, e99. https://doi.org/10.1093/nar/gkad761.

1137 91. van Kempen, M., Kim, S.S., Tumescheit, C., Mirdita, M., Lee, J., Gilchrist, C.L.M.,
1138 Söding, J., and Steinegger, M. (2023). Fast and accurate protein structure search with
1139 Foldseek. Nat. Biotechnol., 1–4. https://doi.org/10.1038/s41587-023-01773-0.

1140 92. Schrödinger, LLC (2015). The PyMOL Molecular Graphics System, Version 2.5.7.

1141 93. Galaxy Community (2024). The Galaxy platform for accessible, reproducible, and
1142 collaborative data analyses: 2024 update. Nucleic Acids Res. *52*, W83–W94.
1143 https://doi.org/10.1093/nar/gkae410.

1144 94. heatmap.2: Enhanced Heat Map. (n.d.).

1145 95. de Jong, A., Kuipers, O.P., and Kok, J. (2022). FUNAGE-Pro: comprehensive web
1146 server for gene set enrichment analysis of prokaryotes. Nucleic Acids Res. *50*, W330–W336.
1147 https://doi.org/10.1093/nar/gkac441.

1148 96. Kumar, S., Stecher, G., Suleski, M., Sanderford, M., Sharma, S., and Tamura, K.
1149 (2024). MEGA12: Molecular Evolutionary Genetic Analysis version 12 for adaptive and
1150 green computing. Mol. Biol. Evol. *41*, msae263. https://doi.org/10.1093/molbev/msae263.

1151 97. Crooks, G.E., Hon, G., Chandonia, J.-M., and Brenner, S.E. (2004). WebLogo: a
1152 sequence logo generator. Genome Res. *14*, 1188–1190. https://doi.org/10.1101/gr.849004.

1153 98. Cartagena, A.J., Banta, A.B., Sathyan, N., Ross, W., Gourse, R.L., Campbell, E.A.,
1154 and Darst, S.A. (2019). Structural basis for transcription activation by Crl through tethering of
1155 σS and RNA polymerase. Proc. Natl. Acad. Sci. U. S. A. *116*, 18923–18927.
1156 https://doi.org/10.1073/pnas.1910827116.

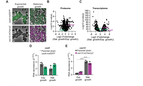
A
Transcriptomic
Proteomic
Transcriptomic
Proteomic
B
Transcriptomic
Proteomic
Transcriptomic
Proteomic
C
Transcriptomic
Proteomic
Transcriptomic
Proteomic
Transcriptomic
Proteomic